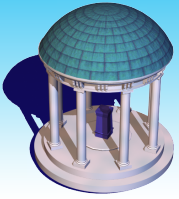


Functional Data Analysis of Big Neuroimaging Data

Hongtu Zhu, Ph.D

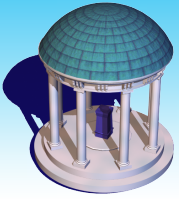
**Department of Biostatistics[†] and Biomedical Research Imaging Center[‡]
The University of North Carolina at Chapel Hill,
Chapel Hill, NC 27599, USA**

Acknowledgement: Some pictures were copied from multiple resources including Suetens (2009), Fass (2008), Dr. Niethammer, Drs. Lindquist, Rowe, Huettel, Wiki, google, gustaf@cb.uu.se, etc.



Big Neuroimaging Data

Is it really big?



Human Brain Project

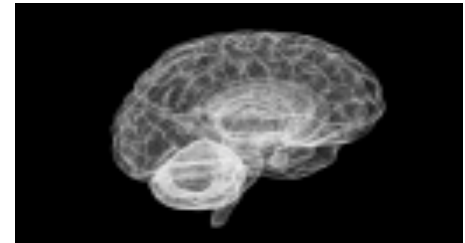
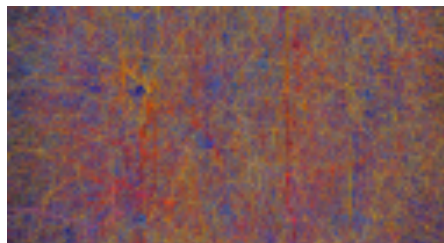
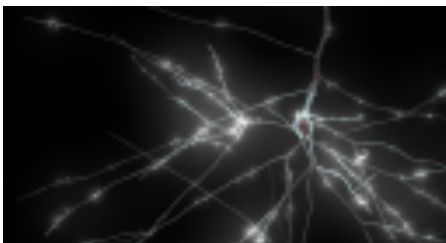
aims to simulate the complete human brain on Supercomputers to better understand how it functions.

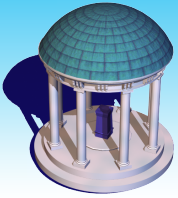


The Brain Research through

Advancing Innovative Neurotechnologies or BRAIN,

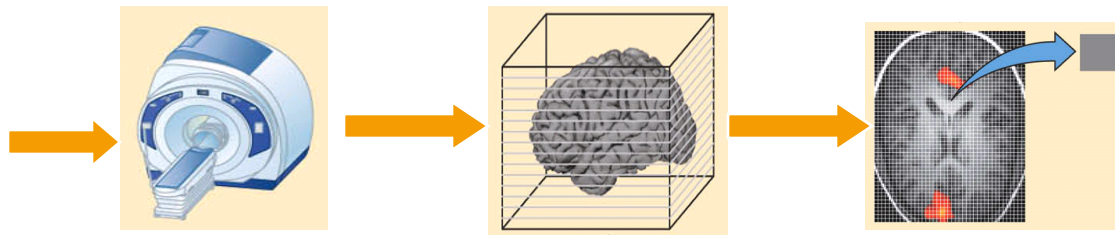
aims to reconstruct the activity of every single neuron as they fire simultaneously in different brain circuits, or perhaps even whole brains.



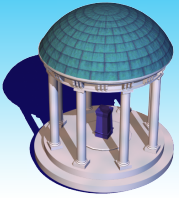


Big Neuroimaging Data

**NIH normal brain development
1000 Functional Connectome Project
Alzheimer's Disease Neuroimaging Initiative
National Database for Autism Research (NDAR)
Human Connectome Project**

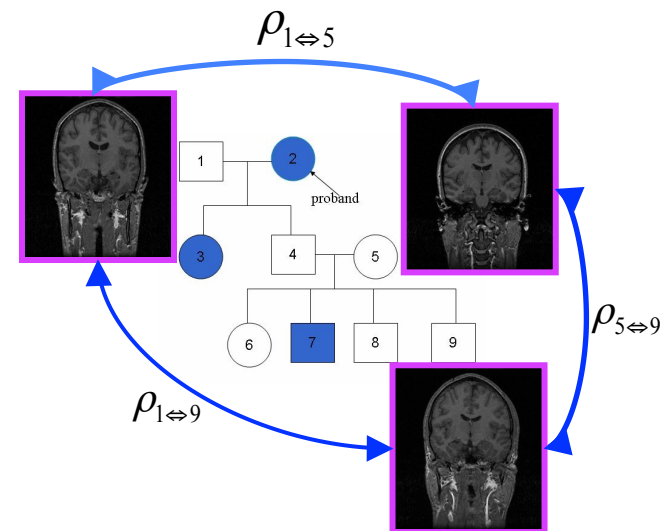
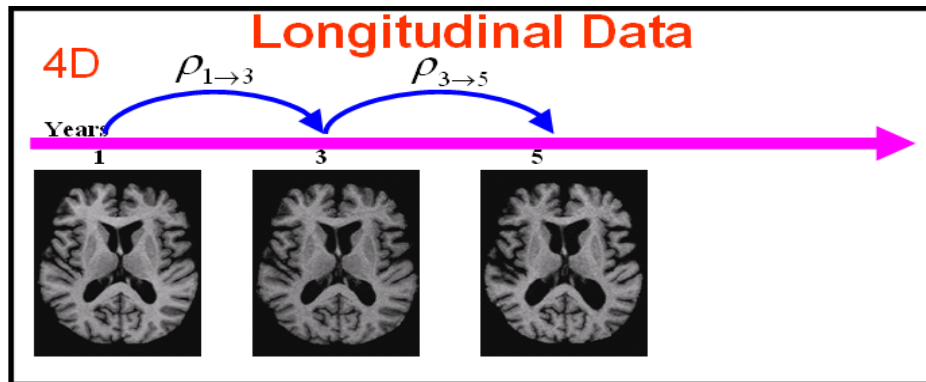


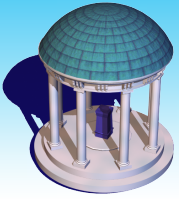
www.guysandstthomas.nhs.uk/.../T/Twins400.jpg



Complex Study Design

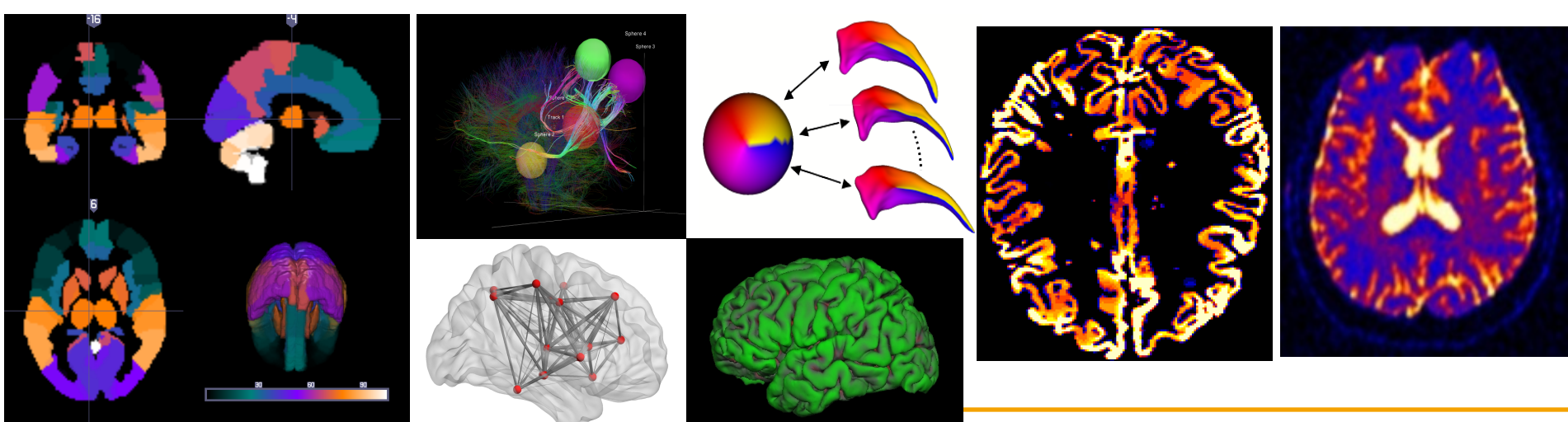
**cross-sectional studies;
clustered studies including
longitudinal and twin/familial studies;**

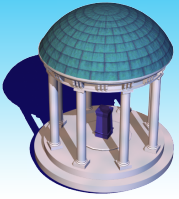




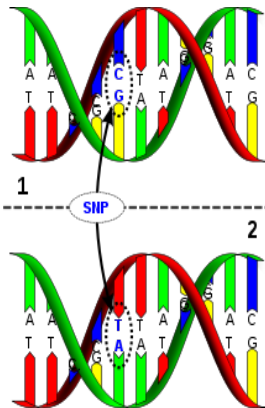
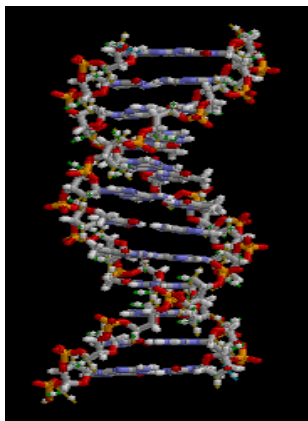
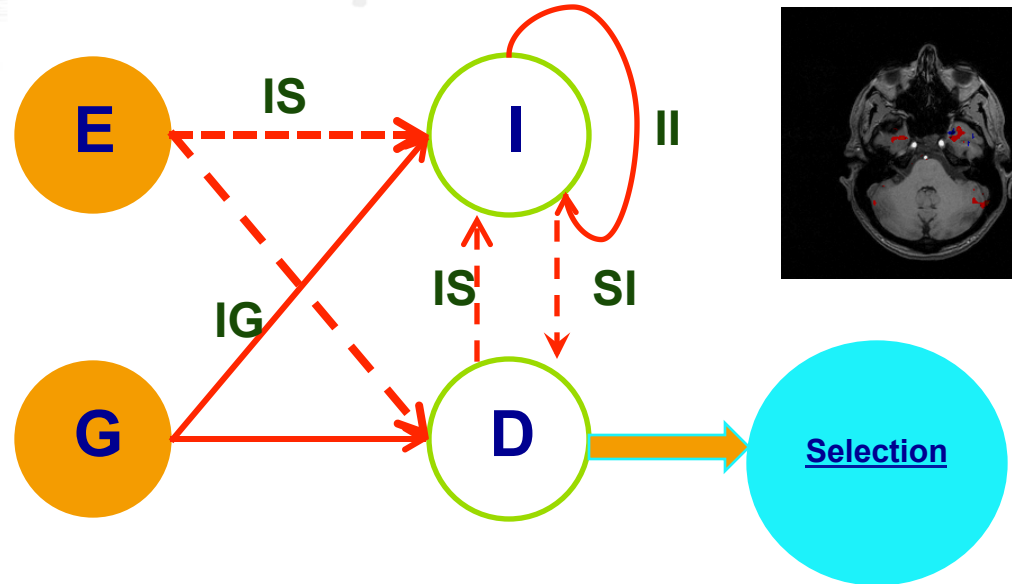
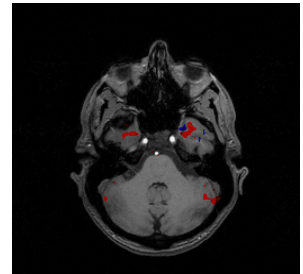
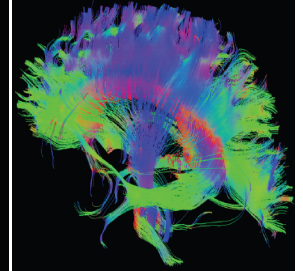
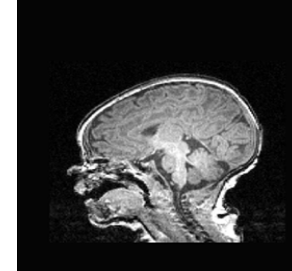
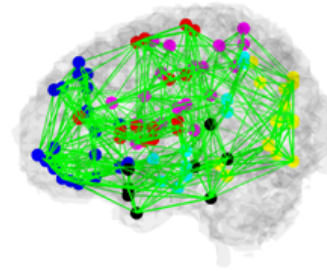
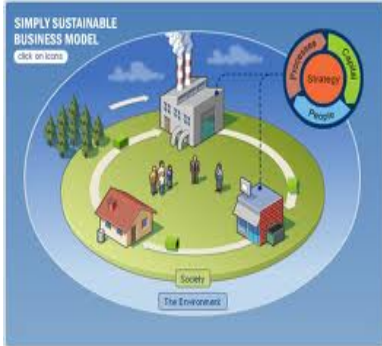
Complex Data Structure

Multivariate Imaging Measures
Smooth Functional Imaging Measures
Whole-brain Imaging Measures
4D-Time Series Imaging Measures

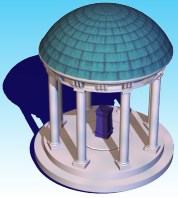




Big Data Integration



http://en.wikipedia.org/wiki/DNA_sequence



Models for Big Data Integration

Image-on-Scalar (IS) model

Image data as response, clinical variables as predictors.

Scalar-on-Image (SI) model

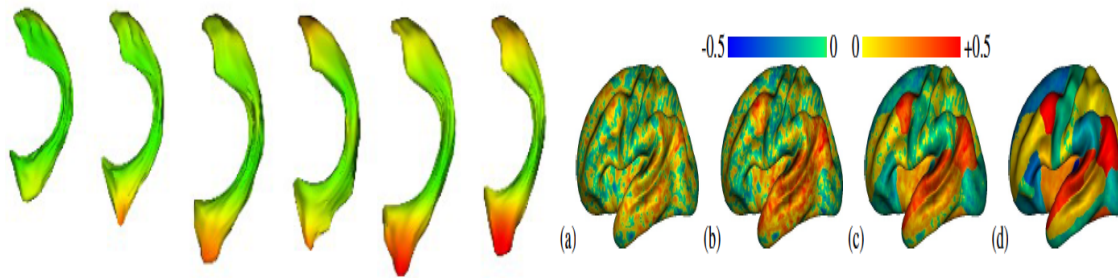
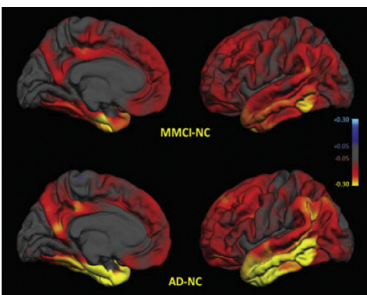
Clinical variables as response, image data as predictors

Image-on-Genetic (IG) model

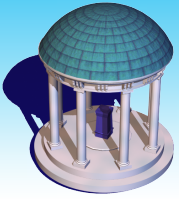
Image data as response, genetic data as predictors

Image-on-Image (II) model

Image data as response, image data as predictors



| | Imaging | Candidate ROI | Many ROI | Voxelwise |
|------------------|---------|---------------|----------|------------|
| Genetics | | | | |
| Candidate SNP | | Imager | Imager | Imager |
| Candidate Gene | | Geneticist | | Geneticist |
| Genome-wide SNP | | Geneticist | | |
| Genome-wide Gene | | Geneticist | | |



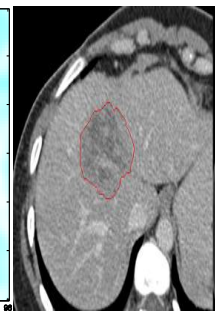
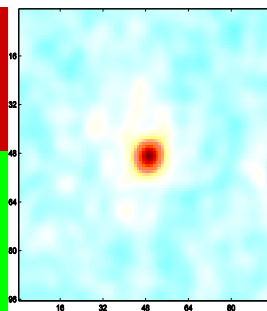
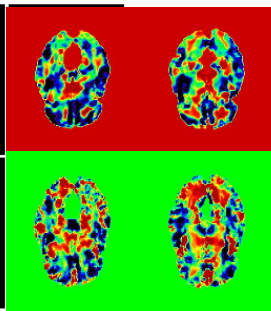
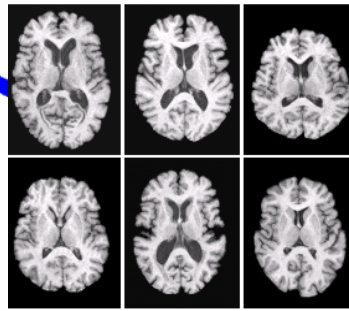
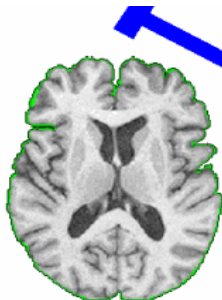
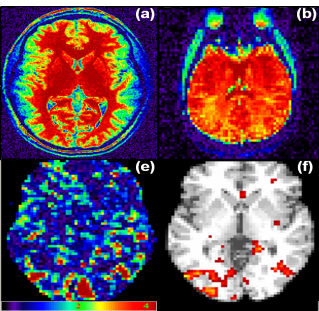
Noisy Imaging Data

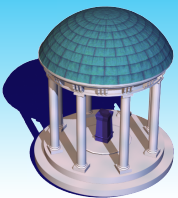
- **Spatial Maps**
- **'Registration'**
- **'Smoothing'**
- **'Correlation'**
- **'Spatial Heterogeneity'**

Estimation

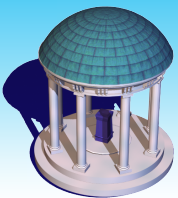
Inference

Prediction





Imaging-on-Scalar Regression



VBA versus FDA

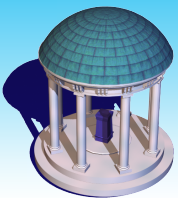
Data $\{(x_i, Y_i) : i = 1, \dots, n\}$ $Y_i = \{Y_i(d_0) : d_0 \in D_0\}$

- **Intrinsic Discrete Approach (VBA)**

$$Y_i = \{Y_i(d_0) : d_0 \in D_0\}$$

- **Intrinsic Functional Approach (FDA)**

$$Y_i(\bullet) = \{Y_i(d) : d \in D\}$$



Functional Data Analysis (FDA)

Big data

$$y_i(d) = x_i^T B(d) + \eta_i(d) \quad \eta_i(\bullet) \sim SP(0, \Sigma_\eta)$$

Hotelling-type Test Statistics T_n^2

Pro:

- Incorporate spatial smoothness and spatial correlation

Con:

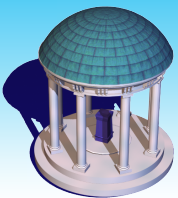
- Computational and theoretical difficulties

$$\bar{Y} = \sum_{i=1}^n Y_i / n \quad S_Y = \sum_{i=1}^n (Y_i - \bar{Y}) \otimes (Y_i - \bar{Y}) / n \quad T_n^2 = n \sup_{\|u\|=1} \frac{\langle \bar{Y}, u \rangle^2}{\langle u, S_Y u \rangle}$$

$$P(T_n^2 = \infty) = 1$$

$$S_Y \rightarrow \alpha(S_Y)$$

$$S_Y \rightarrow \text{diag}(S_Y)$$



High-dimensional Regression Models

Big data

$$Y_i = BX_i + \eta_i \quad \eta_i(\bullet) \sim SP(0, \Sigma_\eta) \quad \dim(Y_i) \gg n$$

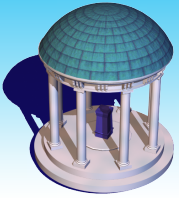
Hotelling-type Test Statistics T_n^2

$$\bar{Y} = \sum_{i=1}^n Y_i / n \quad S_Y = \sum_{i=1}^n (Y_i - \bar{Y})(Y_i - \bar{Y})^T / n \quad T_n^2 = n \sup_{\|u\|=1} \frac{\langle \bar{Y}, u \rangle^2}{\langle u, S_Y u \rangle}$$

$$P(T_n^2 = \infty) = 1$$

$$(\bar{Y}, S_Y) \rightarrow \alpha(Y, S_Y)$$





Voxel Based Analysis (VBA)

Data $\{(x_i, Y_i) : i = 1, \dots, n\}$ $Y_i = \{Y_i(d_0) : d_0 \in D_0\}$

VBA

Stage 0: Gaussian Kernel Smoothing

Stage 1: Model Fitting

$$\prod_{i=1}^n p(Y_i | x_i) = \prod_{i=1}^n \prod_{d \in D_0} p(Y_i(d_0) | x_i, \theta(d_0))$$

Ignore spatial smoothness

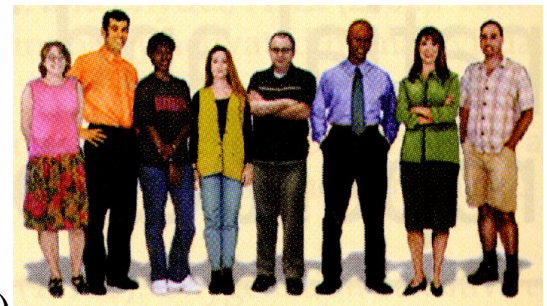
Stage 2: Hypothesis Testing

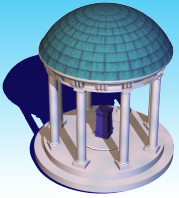
$H_0 : \theta(d) = \theta_*(d)$ for all voxels

$H_1 : \theta(d) \neq \theta_*(d)$ for some voxels

Random Field Theory: functional data and local smoothness

FDR





VBA

Cons

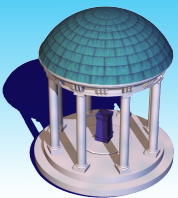
Potential large smoothing errors.

Treat voxels as independent units/images as a collection of independent voxels.

Ignore spatial correlation and smoothness in statistical analysis.

Inaccurate for both Prediction and Estimation.

Decrease statistical power.



VBA Bayesian Extensions

Bayesian Modeling

Spatial smooth prior (MRF) $p(\theta) = p(\{\theta(d_0) : d_0 \in D_0\})$

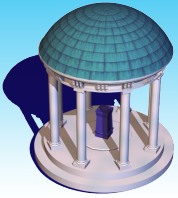
$$p(\theta | Y) \propto \left\{ \prod_{i=1}^n p(Y_i | x_i, \theta) \right\} p(\theta) = \left\{ \prod_{i=1}^n \prod_{d \in D_0} p(Y_i(d) | x_i, \theta(d)) \right\} p(\theta)$$

Pro:

- **Computationally straightforward;**
- **Bayesian inference based on MCMC samples**

Con:

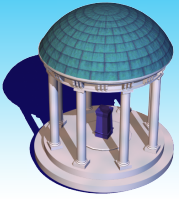
- **Computationally heavy;**
- **Lack of understanding for Bayesian inference tools.**



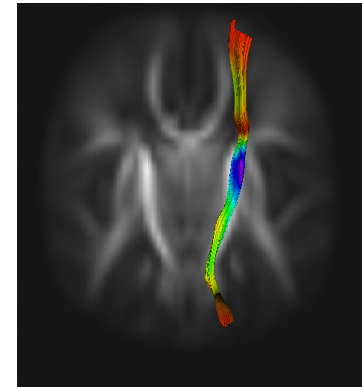
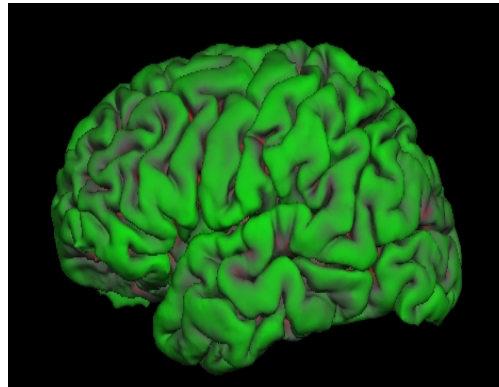
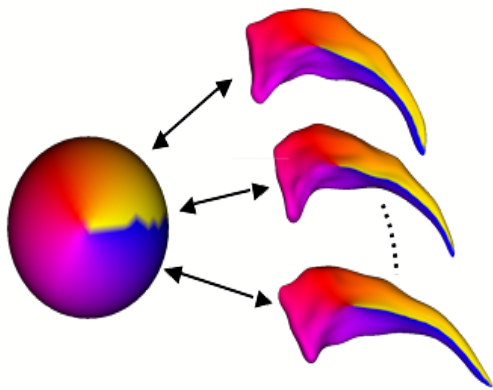
Varying Coefficient Models

Reading materials:

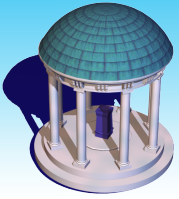
1. [Zhu, H. T.](#), Chen, K. H., Yuan, Y. and Wang, J. L. (2014). Functional Mixed Processes Models for Repeated Functional Data. In submission.
2. Liang, J. L., Huang, C., and [Zhu, H.T.](#) (2014). Functional single-index varying coefficient models. In submission.
3. Yuan, Y., Gilmore, J., Geng, X. J., Styner, M., Chen, K. H., Wang, J. L., and [Zhu, H.T.](#) (2013). A longitudinal functional analysis framework for analysis of white matter tract statistics. *NeuroImage*, in press.
4. Yuan, Y., [Zhu, H.T.](#), Styner, M., J. H. Gilmore., and Marron, J. S. (2013). Varying coefficient model for modeling diffusion tensors along white matter bundles. *Annals of Applied Statistics*. 7(1):102-125..
5. Zhu, H.T., Li, R. Z., Kong, L.L. (2012). Multivariate varying coefficient models for functional responses. *Ann. Stat.* 40, 2634-2666.
6. Hua, Z.W., Dunson, D., Gilmore, J.H., Styner, M., and [Zhu, HT.](#) (2012). Semiparametric Bayesian local functional models for diffusion tensor tract statistics. *NeuroImage*, 63, 460-674.
7. [Zhu, HT.](#), Kong, L., Li, R., Styner, M., Gerig, G., Lin, W. and Gilmore, J. H. (2011). FADTTS: Functional Analysis of Diffusion Tensor Tract Statistics, *NeuroImage*, 56, 1412-1425.
8. [Zhu, H.T.](#), Styner, M., Tang, N.S., Liu, Z.X., Lin, W.L., Gilmore, J.H. (2010). FRATS: functional regression analysis of DTI tract statistics. *IEEE Transactions on Medical Imaging*, 29, 1039-1049.
9. Greven, S., Crainiceanu, C., Caffo, B., Reich, D. (2010). Longitudinal principal component analysis. *E.J.Statist.* 4, 1022-1054.
10. Goodlett, C.B., Fletcher, P. T., Gilmore, J. H., Gerig, G. (2009). Group analysis of dti fiber tract statistics with application to neurodevelopment. *NeuroImage*, 45, S133-S142.
11. Yushkevich, P. A., Zhang, H., Simon, T., Gee, J. C. (2008). Structure-specific statistical mapping of white matter tracts. *NeuroImage*, 41, 448-461.
12. Ramsay, J. O., Silverman, B. W. (2005). *Functional Data Analysis*, Springer-Verlag, New York.



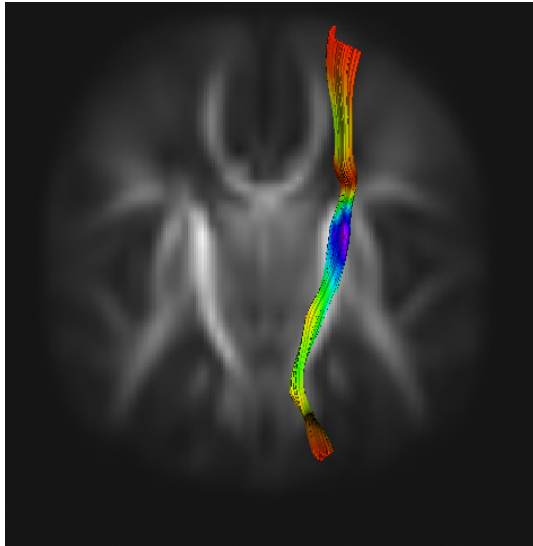
Smoothed Functional Data



Covariates (e.g., age, gender, diagnostic)



DTI Fiber Tract Data



Data

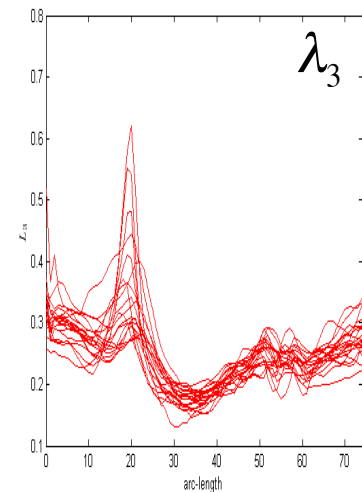
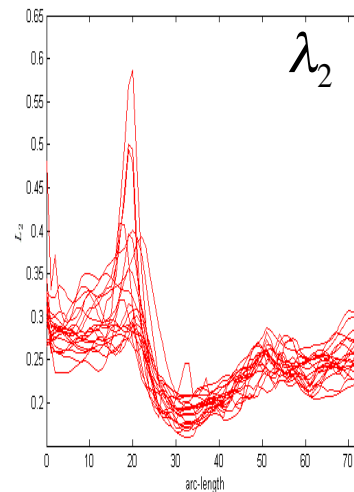
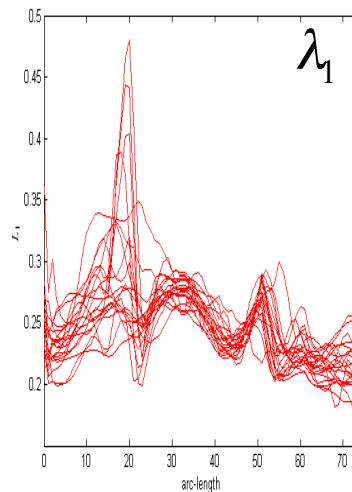
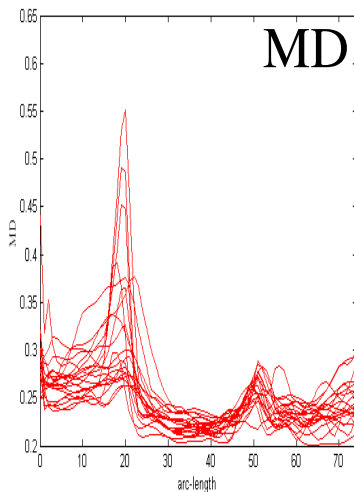
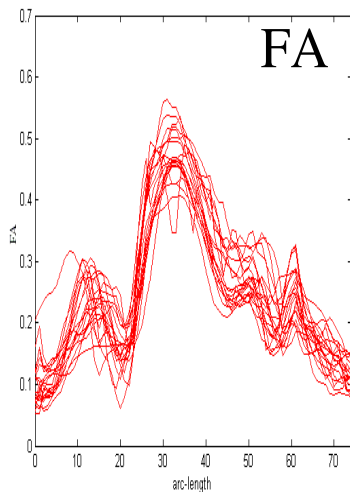
- Diffusion properties (e.g., FA, RA)

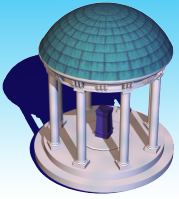
$$Y_i(s_j) = (y_{i,1}(s_j), \dots, y_{i,m}(s_j))^T$$

- Grids $\{s_1, \dots, s_{n_G}\}$

- Covariates (e.g., age, gender, diagnostic)

$$x_1, \dots, x_n$$





MVCM

Decomposition:

$$y_{i,k}(s) = x_i^T B_k(s) + \eta_{i,k}(s) + \varepsilon_{i,k}(s)$$

Coefficients

$$x_1, \dots, x_n$$

Long-range Correlation

$$\eta_{i,k}(\bullet) \sim SP(0, \Sigma_\eta)$$

Short-range Correlation

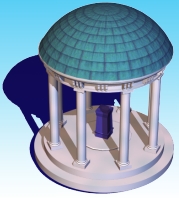
$$\varepsilon_{i,k}(\bullet) \sim SP(0, \Sigma_\varepsilon),$$

Covariance operator:

$$\Sigma_y(s, s') = \Sigma_\eta(s, s') + \Sigma_\varepsilon(s, s')$$

$$\sqrt{n} \{ \text{vec}(\hat{B}(d) - B(d) - 0.5O(H^2)) : d \in D \} \xrightarrow{L} G(0, \Sigma_B(d, d'))$$

Zhu, Li, and Kong (2012). AOS

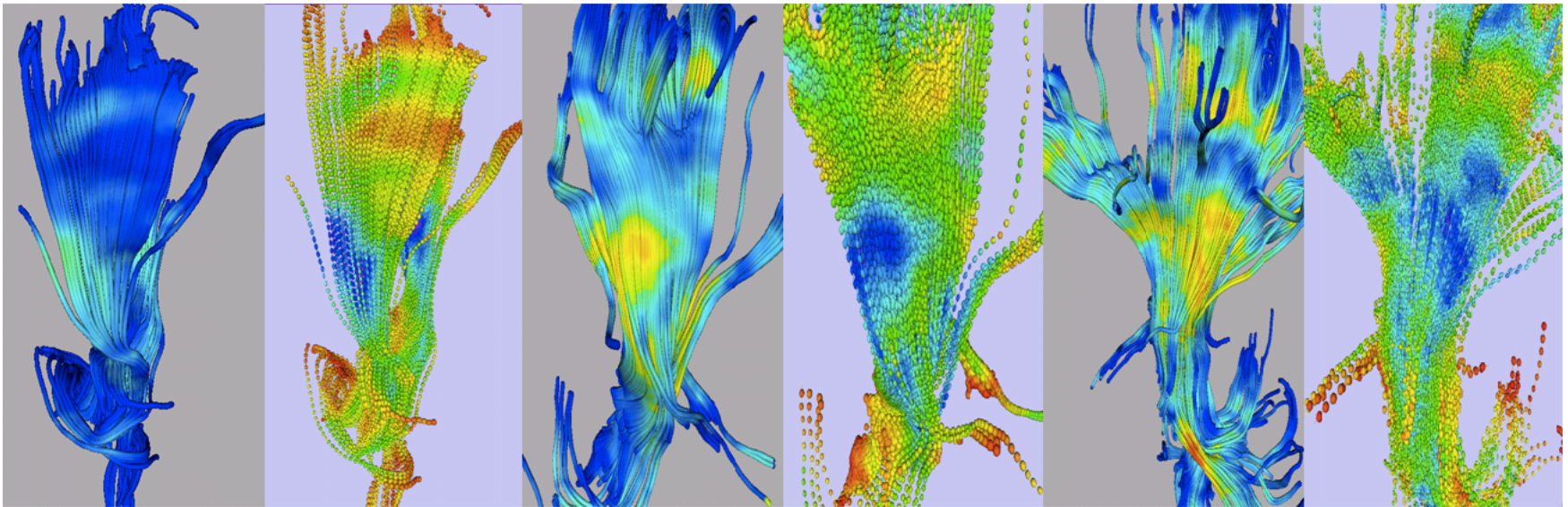


Motivation

Diffusion Tensor Tract Statistics

FA

Tensor



(a1)

(b1)

(a2)

(b2)

(a3)

(b3)

2 week

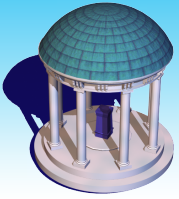
2 week

1 year

1 year

2 year

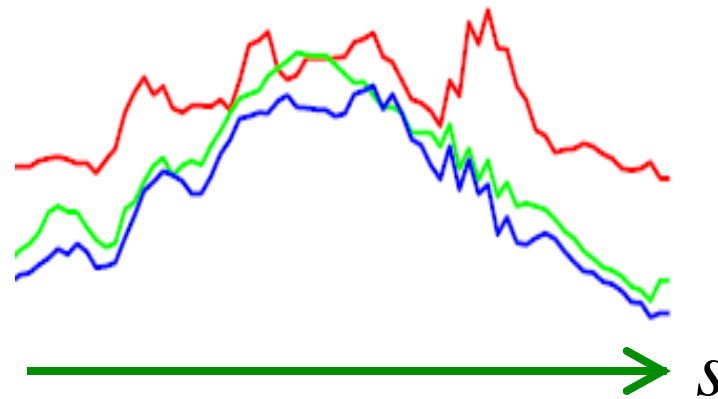
2 year



Longitudinal Extensions

Longitudinal Data

t ↑ $y_i(s, t_3)$
 $y_i(s, t_2)$
 $y_i(s, t_1)$



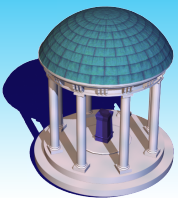
Spatial-temporal Process

Functional Mixed Effect Models

$$y_i(s, t) = x_i(t)^T B(s) + z_i(t)^T \xi_i(s) + \eta_i(s, t) + \varepsilon_i(s, t)$$

Objectives:

Dynamic functional effects of covariates of interest on functional response.



FMEM

Decomposition:

$$y_i(d, t) = x_i(t)^T B(d) + z_i(t)^T \xi_i(d) + \eta_i(d, t) + \varepsilon_i(d, t)$$

Global Noise Components

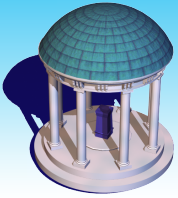
Local Correlated Noise

$$\eta_i(\bullet, \bullet) \sim SP(0, \Sigma_\eta), \quad \xi_i(\bullet) \sim SP(0, \Sigma_\xi) \quad \varepsilon_i(\bullet) \sim SP(0, \Sigma_\varepsilon),$$

$$\sqrt{n} \{ \text{vec}(\hat{B}(d) - B(d) - 0.5O(H^2)) : d \in D \} \xrightarrow{L} G(0, \Sigma_B(d, d'))$$

Ying et al. (2014). NeuroImage.

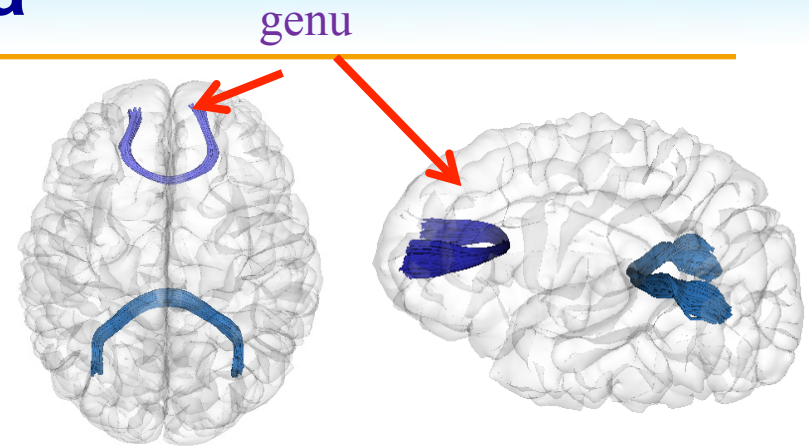
Zhu, Chen, Yuan, and Wang (2014). Arxiv.



Real Data

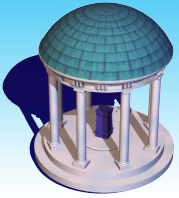
| | |
|----------------------------------|---------------------|
| Gender: Male/Female | 83/54 |
| Gestational age at birth (weeks) | 38.67 ± 1.74 |
| Age at scan 1 (days) | 297.89 ± 13.90 |
| Age at scan 2 (days) | 655.34 ± 24.00 |
| Age at scan 3 (days) | 1021.70 ± 28.26 |
| Number of Gradient directions | |
| dir6/dir42 at scan 1 | 80/24 |
| dir6/dir42 at scan 2 | 59/44 |
| dir6/dir42 at scan 3 | 42/49 |

| | |
|--------------------------------|----|
| Available scans | N |
| Neonate scan only | 1 |
| 1 year scan only | 2 |
| 2 year scan only | 3 |
| Neonate + 1 year scan | 43 |
| Neonate + 2 year scan | 30 |
| 1 year + 2 year scan | 28 |
| Neonate + 1 year + 2 year scan | 30 |

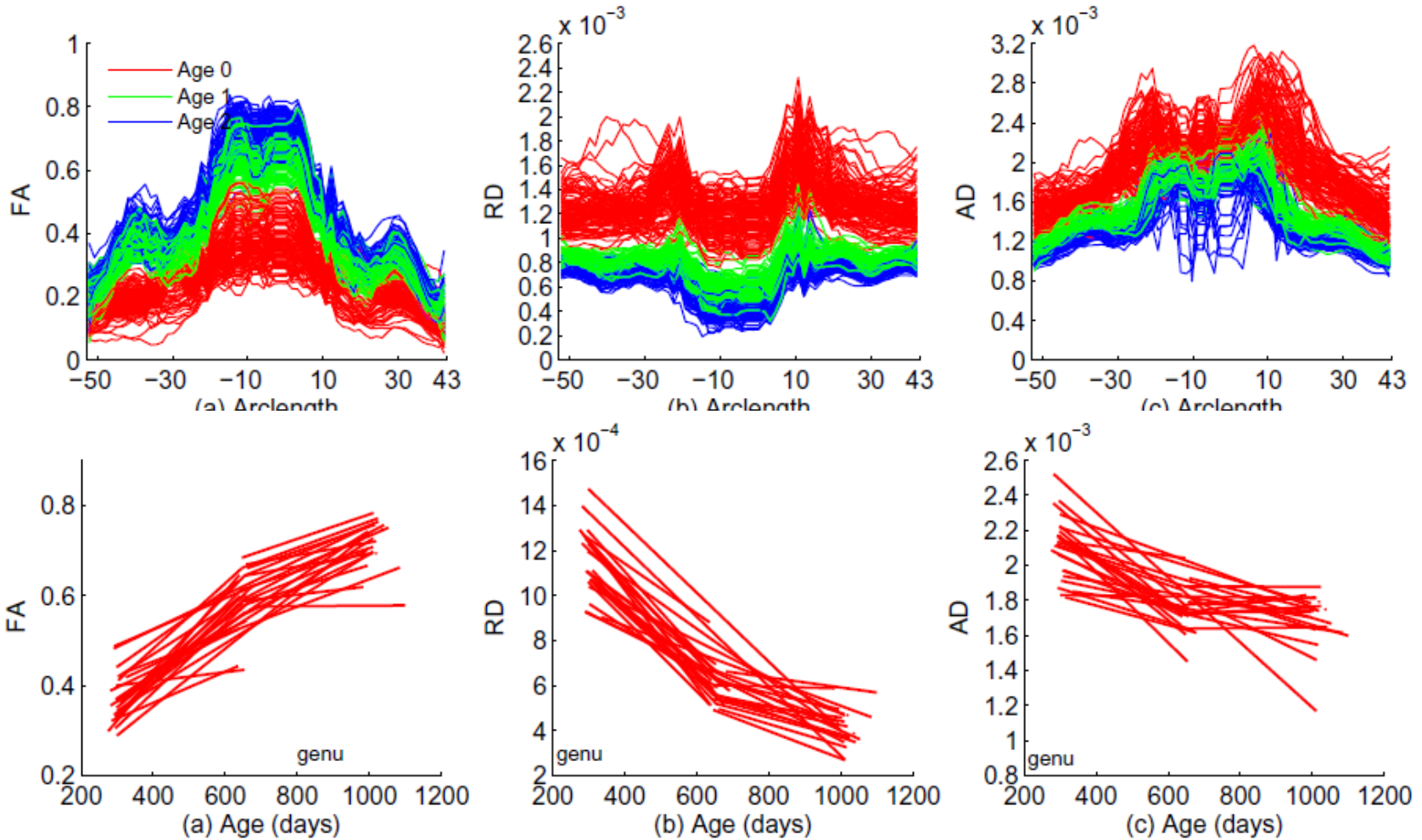


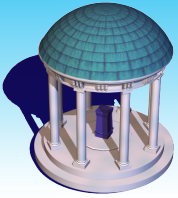
DTImaging parameters:

- **TR/TE = 5200/73 ms**
- **Slice thickness = 2mm**
- **In-plane resolution = $2 \times 2 \text{ mm}^2$**
- **$b = 1000 \text{ s/mm}^2$**
- **One reference scan $b = 0 \text{ s/mm}^2$**
- **Repeated 5 times when 6 gradient directions applied.**

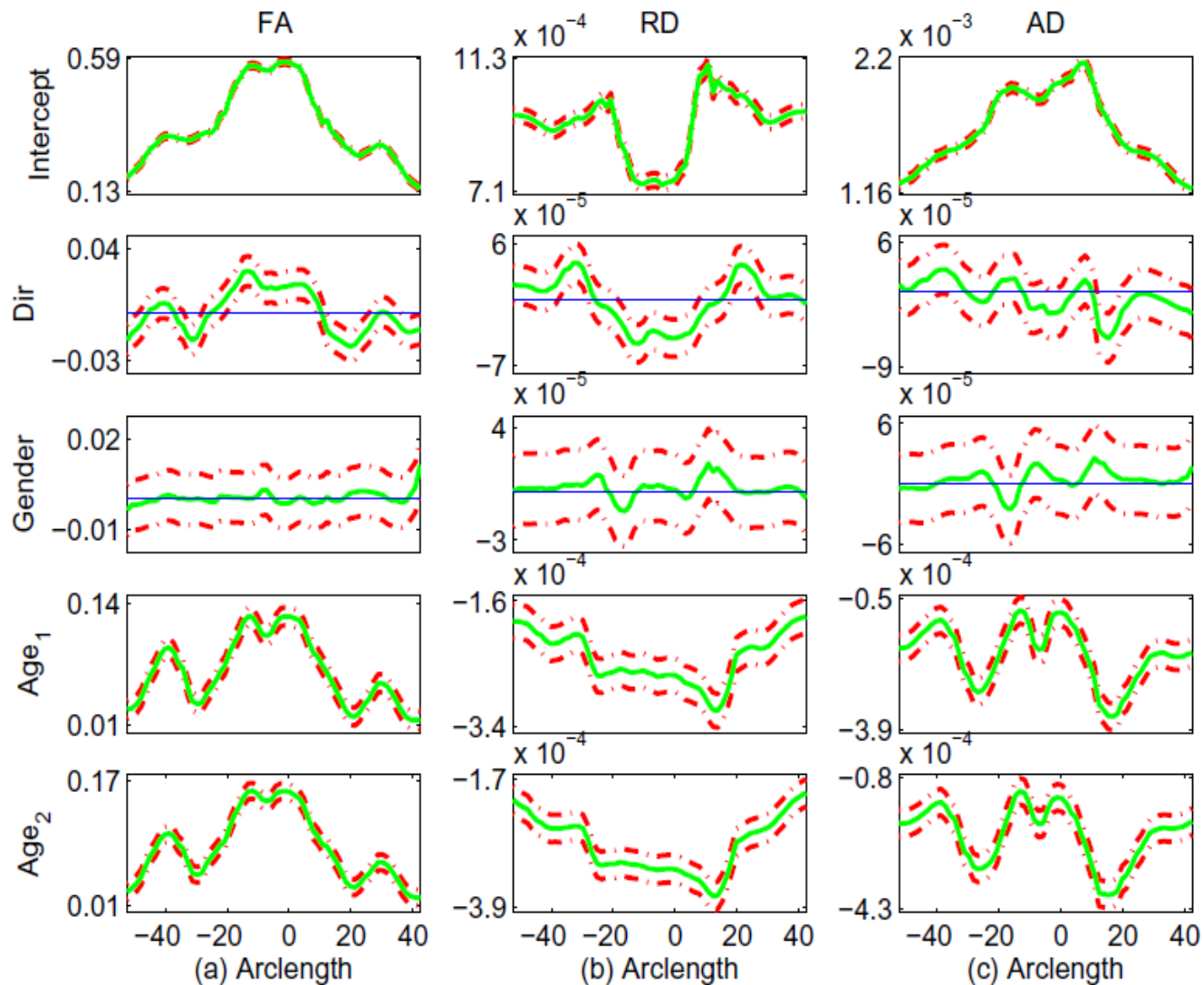


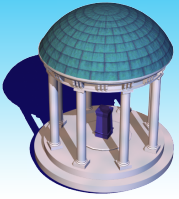
Real Data





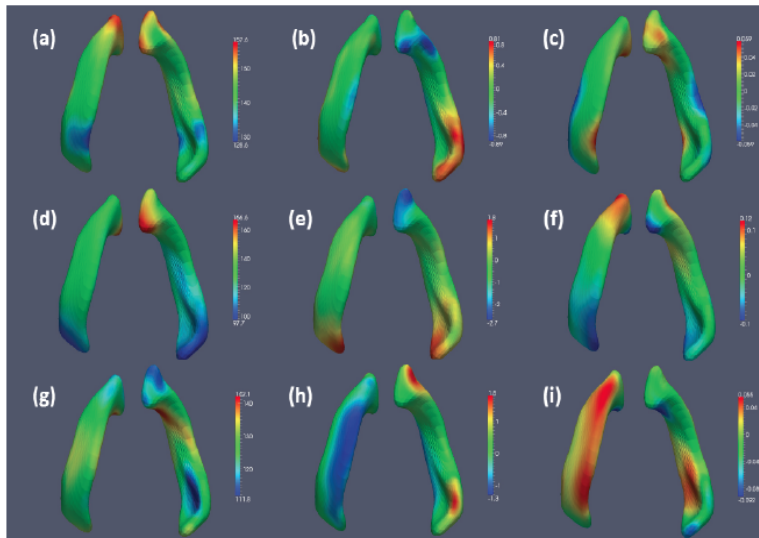
Real Data Analysis Results





Prediction

$$y_{i,k}(s) =$$



$$f(x_i, B_k(s) + \eta_{i,k}(s))$$

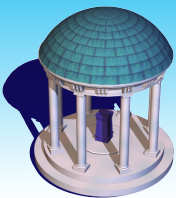
Long-range Correlation

$$+ \varepsilon_{i,k}(s)$$

Small-range Correlation

Missing Big Data???

Hyun, J.W., Li, Y. M., J. H. Gilmore, Z. Lu, M. Styner, H. Zhu (2014) NeuroImage

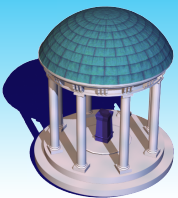


Real Data

Table 3: rtMSPE for the surface data of the left lateral ventricle

| Missingness | | VWLM | GLM+fPCA | SGPP |
|-------------|--------------|--------|----------|--------|
| 10% | x-coordinate | 1.9272 | 0.9810 | 0.0738 |
| | y-coordinate | 2.2448 | 1.3455 | 0.1067 |
| | z-coordinate | 2.1554 | 1.1753 | 0.0926 |
| 30% | x-coordinate | 1.9337 | 1.0197 | 0.1156 |
| | y-coordinate | 2.2655 | 1.3827 | 0.1657 |
| | z-coordinate | 2.1906 | 1.2069 | 0.1446 |
| 50% | x-coordinate | 1.9263 | 1.0294 | 0.1615 |
| | y-coordinate | 2.2012 | 1.3471 | 0.2204 |
| | z-coordinate | 2.1862 | 1.1830 | 0.1924 |

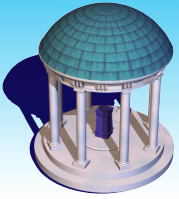
Prediction Accuracy is much improved



Multiscale Adaptive Regression Models

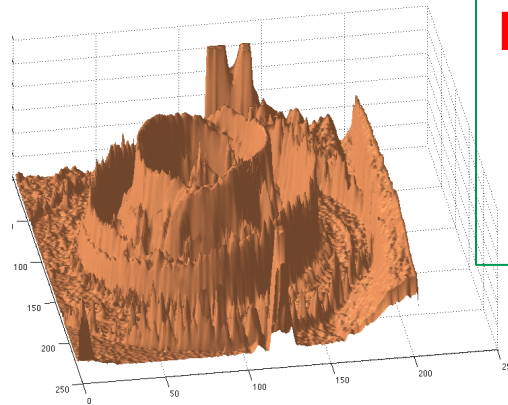
Reading materials:

1. Zhu, HT., Fan, J., and Kong, L. (2014). Spatial varying coefficient model and its applications in neuroimaging data with jump discontinuity. *JASA*, in press.
2. Li, YM, John Gilmore, JA Lin, Shen DG, Martin, S., Weili Lin, and Zhu, HT. (2013). Multiscale adaptive generalized estimating equations for longitudinal neuroimaging data. *NeuroImage*, 72, 91-105.
3. Li, YM, John Gilmore, JP Wang, M. Styner, Weili Lin, and Zhu, HT. (2012). Two-stage spatial adaptive analysis of twin neuroimaging data. *IEEE Transactions on Medical Imaging*. 31, 1100-12.
4. Skup, M., Zhu, H.T., and Zhang HP. (2012). Multiscale adaptive marginal analysis of longitudinal neuroimaging data with time-varying covariates. *Biometrics*, 68(4):1083-1092.
5. Shi, XY, Ibrahim JG, Styner M., Yimei Li, and Zhu, HT. (2011). Two-stage adjusted exponential tilted empirical likelihood for neuroimaging data. *Annals of Applied Statistics*, 5, 1132-1158.
6. Li, YM, Zhu HT, Shen DG, Lin WL, Gilmore J, and Ibrahim JG. (2011). Multiscale adaptive regression models for neuroimaging data. *JRSS, Series B*, 73, 559-578.
7. Polzehl, Jörg; Voss, Henning U.; Tabelow, Karsten. Structural adaptive segmentation for statistical parametric mapping. *NeuroImage*, 52 (2010) pp. 515--523.
8. Polzehl, J. and Spokoiny, V. G. (2006). Propagation-separation approach for local likelihood estimation. *Probability Theory and Related Fields*, 135, 335-362.
9. J. Polzehl, V. Spokoiny. (2000) *Adaptive Weights Smoothing with applications to image restoration*. J. R. Stat. Soc. Ser. B Stat. Methodol., 62 pp. 335--354.



Piecewise Smooth Data

Mathematics.



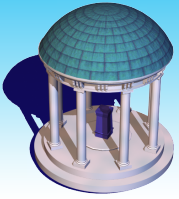
**Noisy Piecewise Smooth
Functions
with Unknown
Jumps and Edges**

Image is the point or set of points in the range corresponding to a designated point in the domain of a given function.

▲ Ω is a compact set. $\tilde{x} \in \Omega \subseteq \mathbb{R}^k$

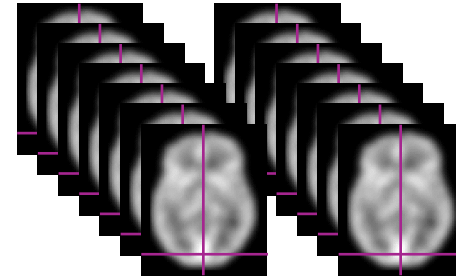
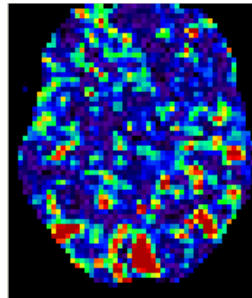
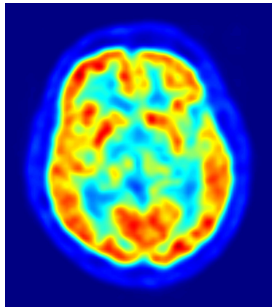
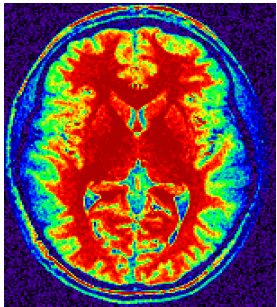
➔ $f(\tilde{x}) \in M \subseteq \mathbb{R}^m$ $f : \Omega \rightarrow M \subseteq \mathbb{R}^m$

★ $\int_{\Omega} \|f(\tilde{x})\|^k d\tilde{x} < \infty$ for some $k > 0$



Neuroimaging Data with Discontinuity

Noisy Piecewise Smooth Function with Unknown Jumps and Edges

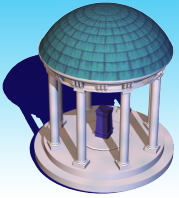


Subject1

Subject2



Covariates (e.g., age, gender, diagnostic, stimulus)



SVCM

Decomposition:

$$y_i(d) = f(x_i, B(d) + \eta_i(d)) + \varepsilon_i(d), d \in D$$

Piecewise Smooth
Varying Coefficients

$$B(d) \in L^K$$

Long-range Correlation

$$\eta_{ij}(\bullet) \sim SP(0, \Sigma_\eta)$$

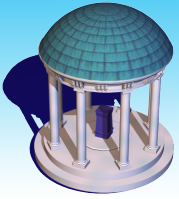
Short-range Correlation

$$\varepsilon_{ij}(\bullet) \sim SP(0, \Sigma_\varepsilon),$$

3D volume/
2D surface

Covariance operator:

$$\Sigma_y(d, d') = \Sigma_\eta(d, d') + \Sigma_\varepsilon(d, d')$$

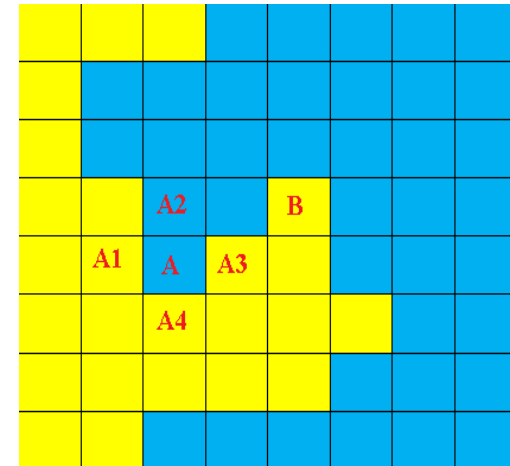
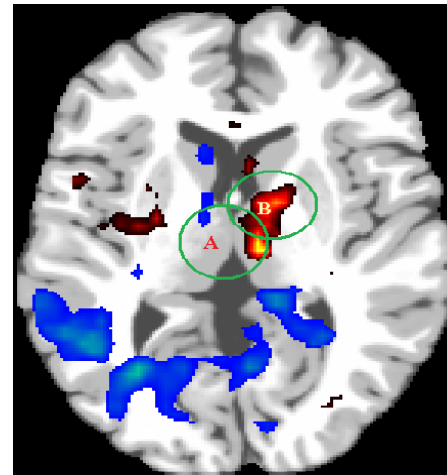


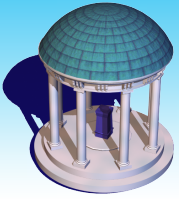
SVCM

Cartoon Model

$$B_k(d)$$

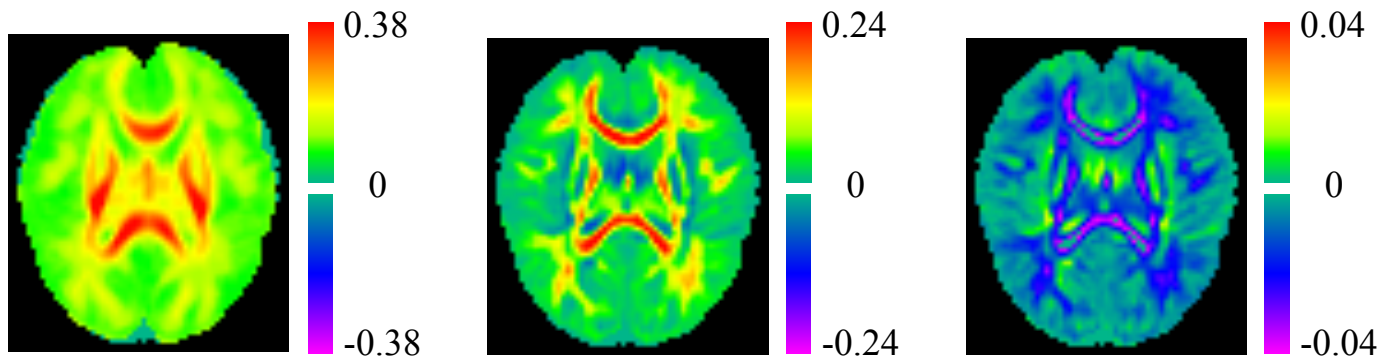
- **Disjoint Partition** $D = \cup_{l=1}^L D_l$ and $D_l \cap D_{l'} = \phi$
- **Piecewise Smoothness: Lipschitz condition**
- **Smoothed Boundary**
- **Local Patch**
- **Degree of Jumps**

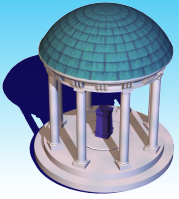




Challenging Issues

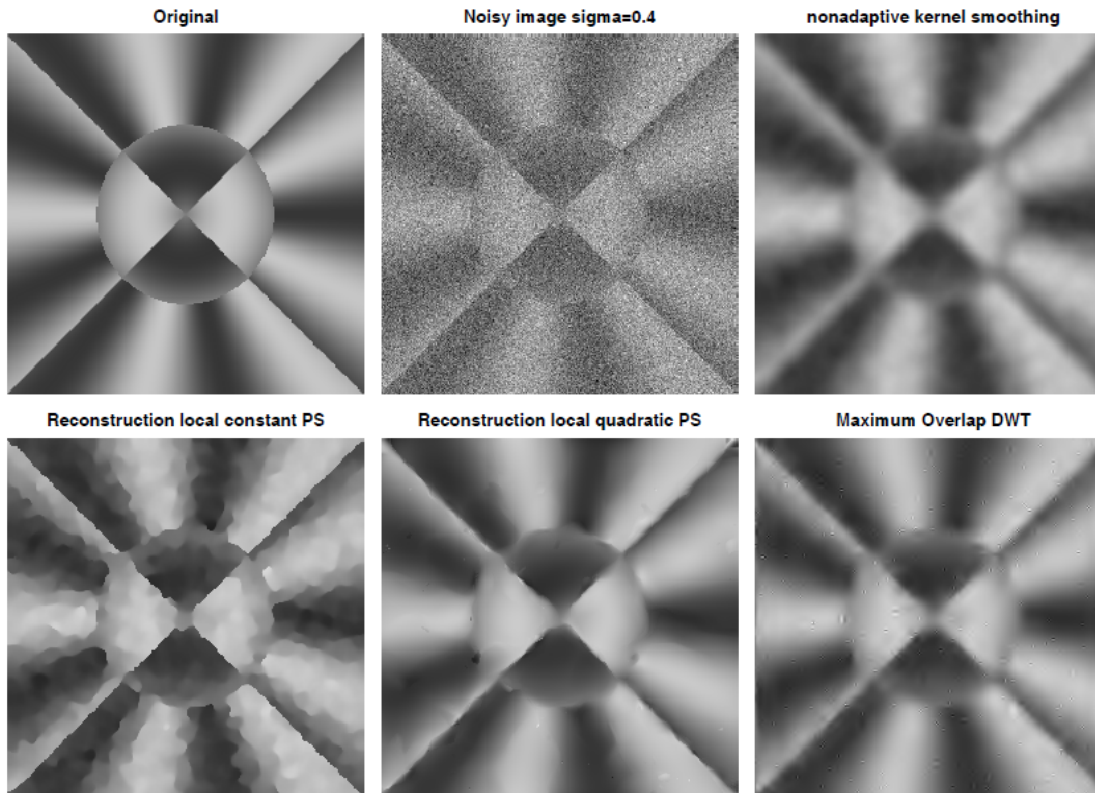
- Smoothing coefficient images, while preserving unknown boundaries
- Different patterns in different coefficient images
- Calculating standard deviation images
- Asymptotic theory





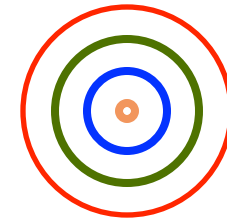
Smoothing Methods

Propagation-Separation Method J. Polzehl and V. Spokoiny, (2000,2005)



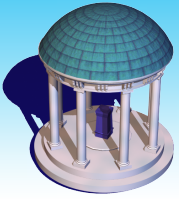
Features

- Increasing Bandwidth



$$0 < h_0 < h_1 < \dots < h_S = r_0$$

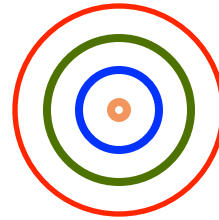
- Adaptive Weights
- Adaptive Estimates



Smoothing Methods

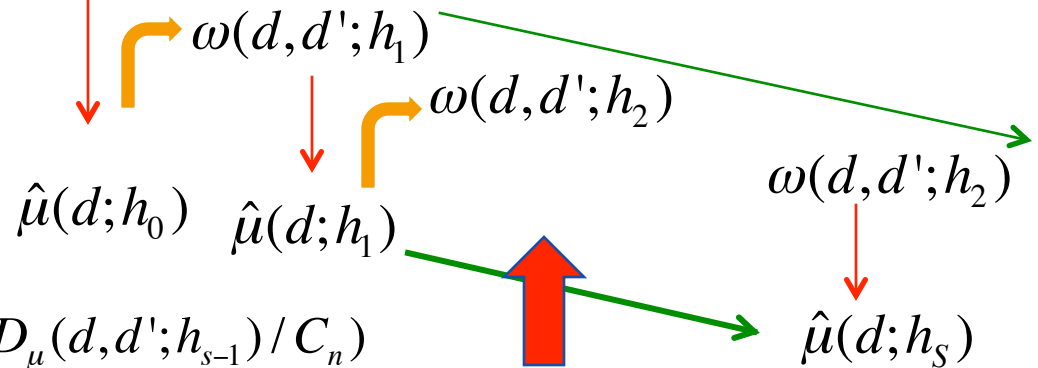
MARM

At each voxel d



$$0 < h_0 < h_1 < \dots < h_S = r_0$$

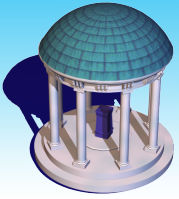
- Increasing Bandwidth
- Adaptive Weights
- Adaptive Estimates



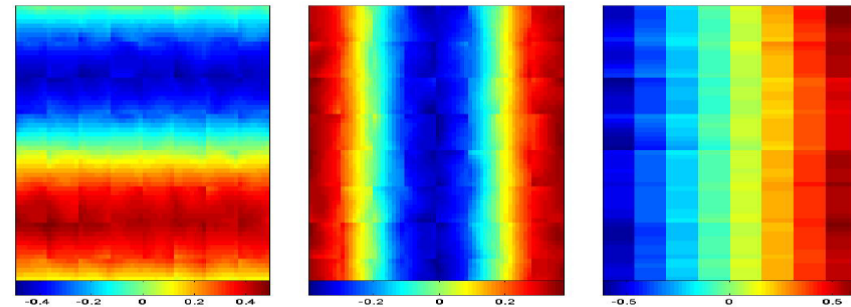
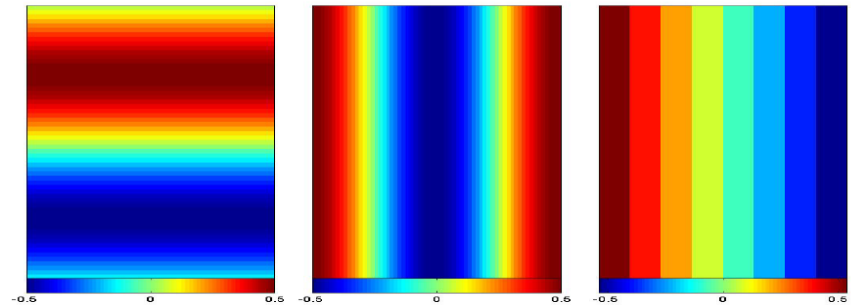
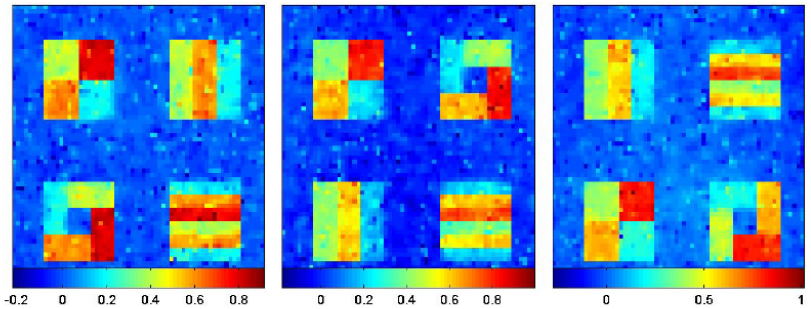
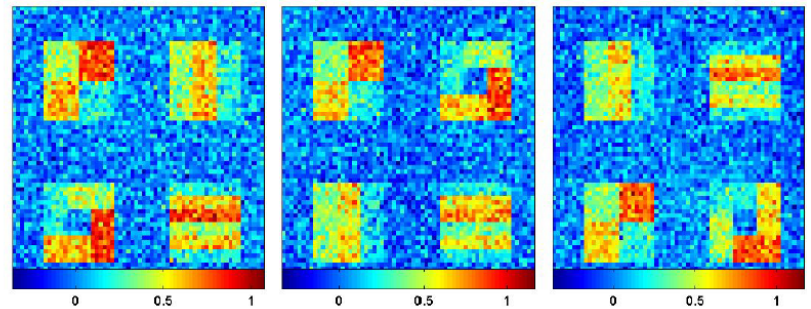
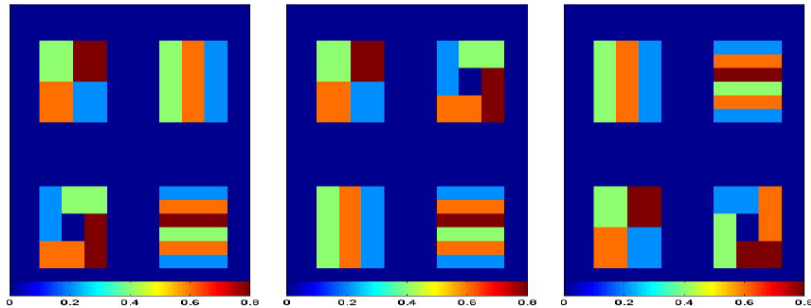
$$\omega(d, d'; h_s) = K_{loc}(\|d - d'\|/h_s)K_{st}(D_\mu(d, d'; h_{s-1})/C_n)$$

$$D_\mu(d, d'; h_{s-1}) = \rho(\hat{\mu}(d; h_{s-1}), \hat{\mu}(d'; h_{s-1}))$$

Stopping Rule

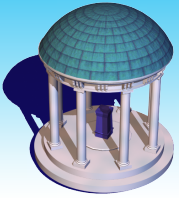


Simulation



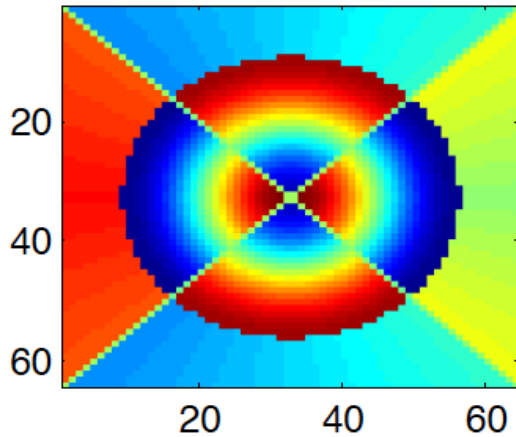
From left to right: $\psi_1(d)$, $\psi_2(d)$, and $\psi_3(d)$.

From up to down: initial and adaptive estimates; left to right: $\beta_1(d)$, $\beta_2(d)$, and $\beta_3(d)$.

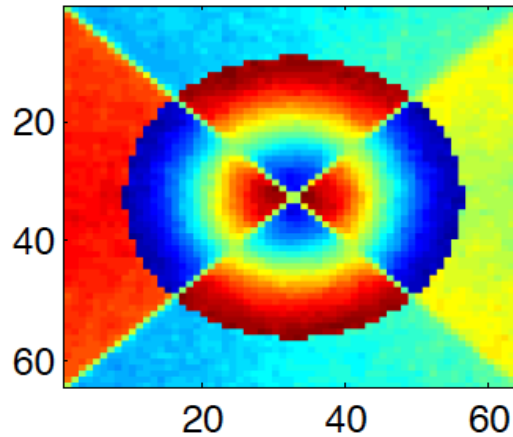


Simulation

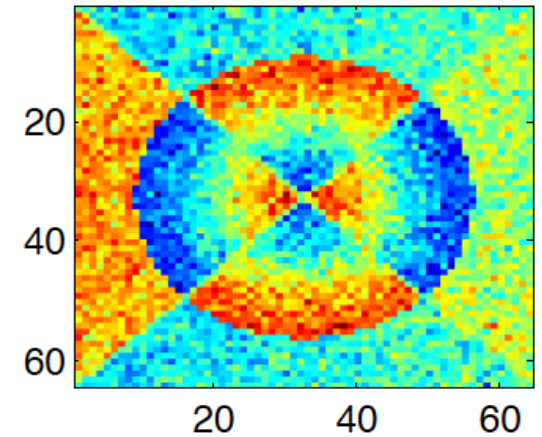
True Image



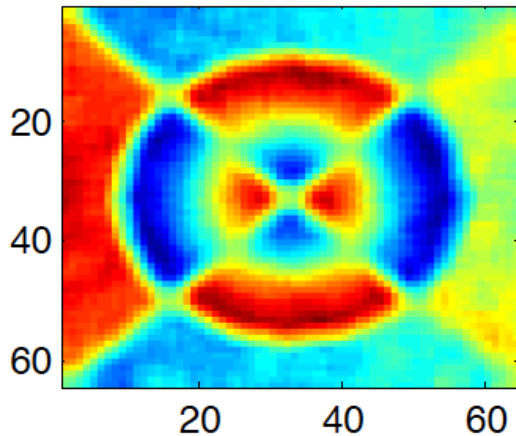
SVCM



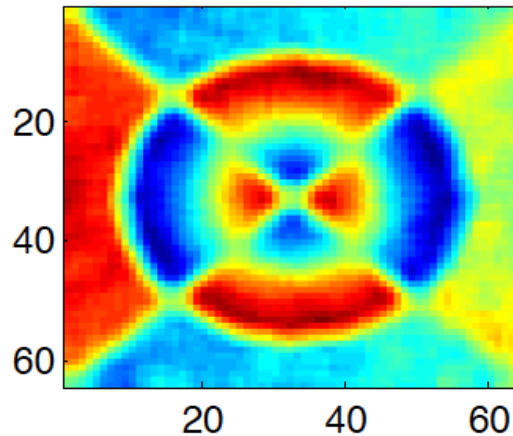
Initial Estimate in SVCM



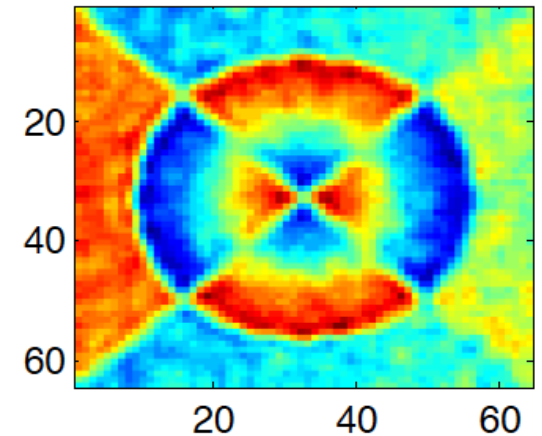
Estimate with LF and $r=0$

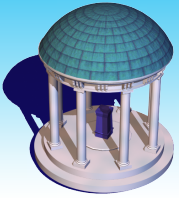


Estimate with LF and $r=1$



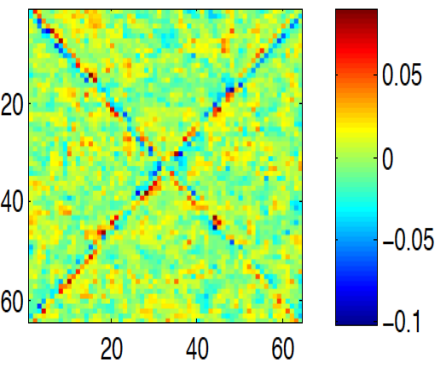
Estimate with LF and $r=2$



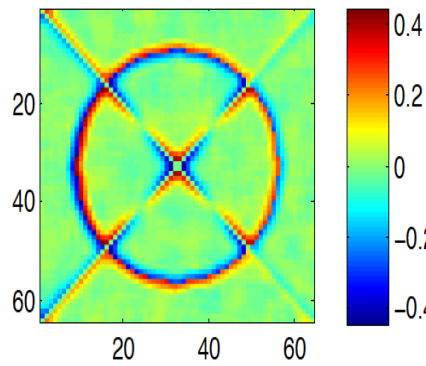


Simulation

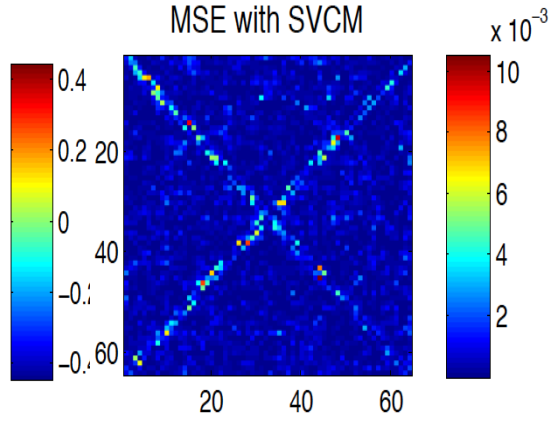
Bias with SVCM



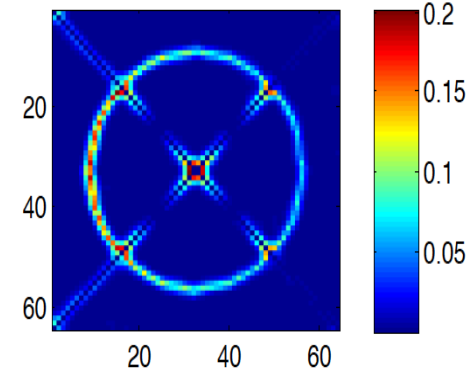
Bias with LF and r=0



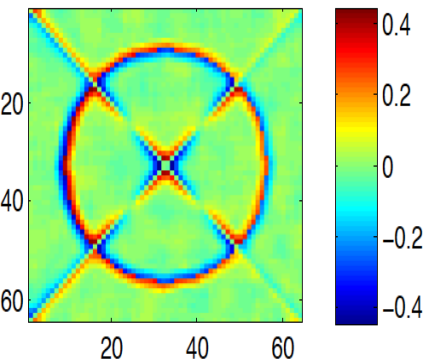
MSE with SVCM



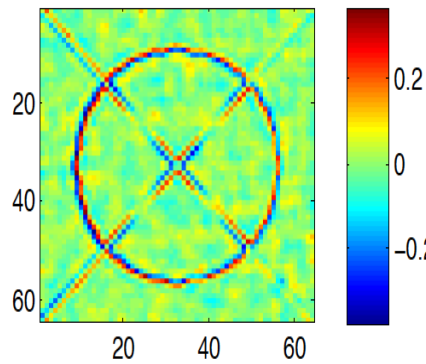
MSE with LF and r=0



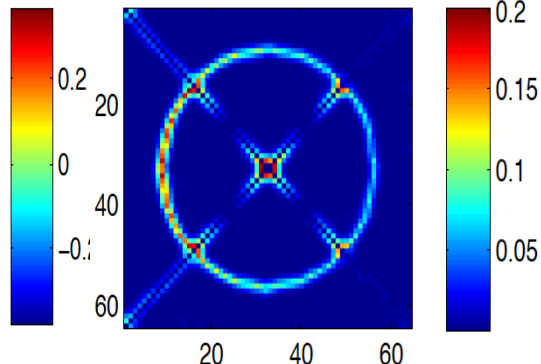
Bias with LF and r=1



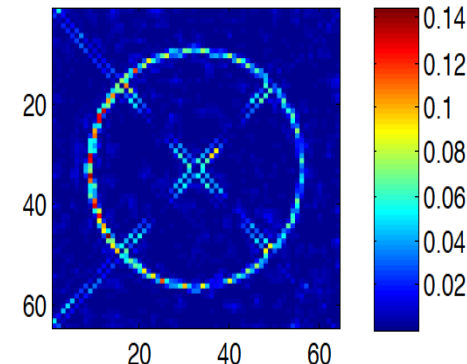
Bias with LF and r=2

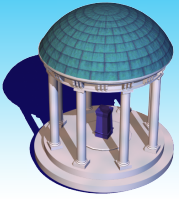


MSE with LF and r=1

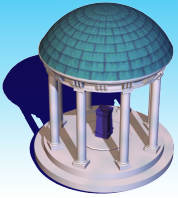


MSE with LF and r=2





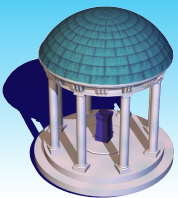
Scalar-on-Imaging Regression



Scalar-on-Image Models

Reading materials:

1. Miranda, M. F., Zhu, H.T. and Ibrahim, J. G. (2014). Bayesian partial supervised tensor decomposition with applications in Neuroimaging data analysis.
2. Yang, H., Zhu, H. T., and Ibrahim, J. G. (2014). Multiscale projection model in RKHS.
3. Zhu, H. T. and Shen, D. (2014). Multiscale Weighted PCA for Imaging Prediction.
4. Guo, R.X., Ahye M., and Zhu, H. (2014). Spatially weighted PCA for imaging classification. *JCGS*. In revision.
5. Zhou, H., Li, L., and Zhu, H. (2013). Tensor regression with applications in Neuroimaging data analysis. *JASA*. In press.
6. Cuingnet, R., Glaunes, J. A., Chupin, M., Benali, H., Colliot, O., and ADNI. (2012). Spatial and anatomical regularization of SVM: a general framework for neuroimaging data. *IEEE PAMI*. In press.
7. Cai, T. & Yuan, M. (2012). Minimax and adaptive prediction for functional linear regression. *JASA*. 107, 1201-1216.
8. Fan, J. and Lv, J. (2010). A selective overview of variable selection in high-dimensional feature space. *Statistica Sinica*, 20, 101-148.
9. Li, B., Kim, M. K., and Altman, N. (2010). On dimension folding of matrix or array valued statistical objects. *Ann. Stat.*, 38, 1097-1121.
10. Reiss, P. T., and Ogden, R. T. (2007). Functional principal component regression and functional partial least squares. *Journal of the American Statistical Association* 102, 984–996.
11. Bair, E., Hastie, T., Paul, D. and Tibshirani, R. (2006). Prediction by supervised principal components. *JASA*. 101, 119-137.
12. Ramsay, J.O. and Silverman, B.W. (2005). *Functional Data Analysis*, 2nd Edition. Springer, New York.
13. James, G. (2002). Generalized linear models with functional predictor variables. *JRSSB*. 64, 411-432.
14. Tibshirani, Robert (1996). Regression shrinkage and selection via the lasso. *JRSSB*. 58, 267-288.



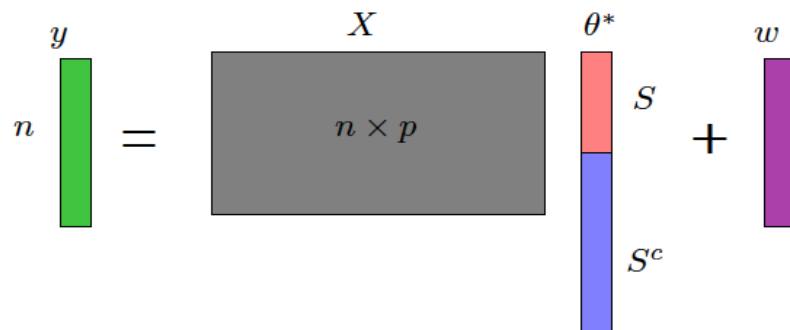
HRM versus FRM

Data $\{(y_i, X_i) : i = 1, \dots, n\}$ $X_i = \{X_i(d) : d \in D\}$

$$y_i = \langle X_i, \theta \rangle + \varepsilon_i$$

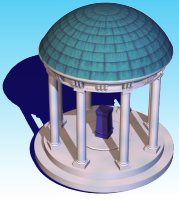
Strategy 1: Discrete Approach

(High-dimension Regression Model (HRM))



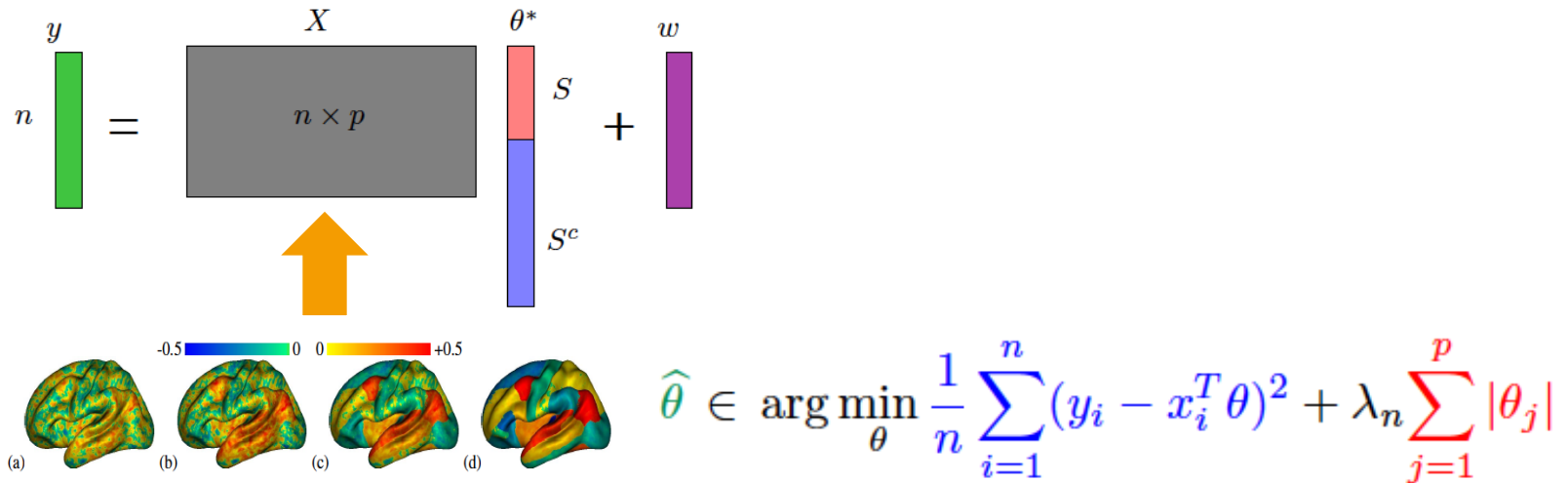
Strategy 2: Functional Regression Model (FRM)

$$y_i = \theta_0 + \int_D \theta(d) X_i(d) m(d) + \varepsilon_i$$



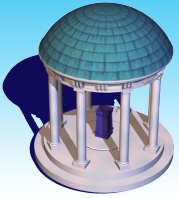
High-dimension Regression Model

Approach 1: Regularization Methods



Key Conditions:

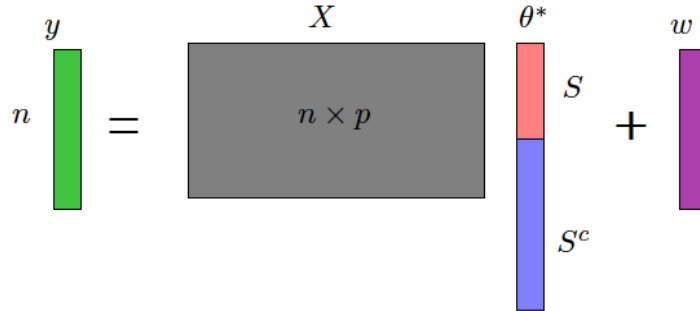
- Sparsity of S
- Restricted null-space property for design matrix X



High-dimension Regression Model

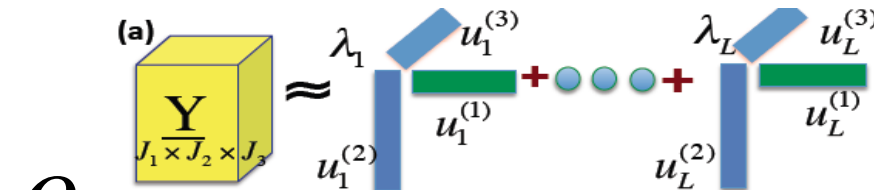
Tensor Structure:

- Ultra-high dimensionality (256^3)
- Spatial structure

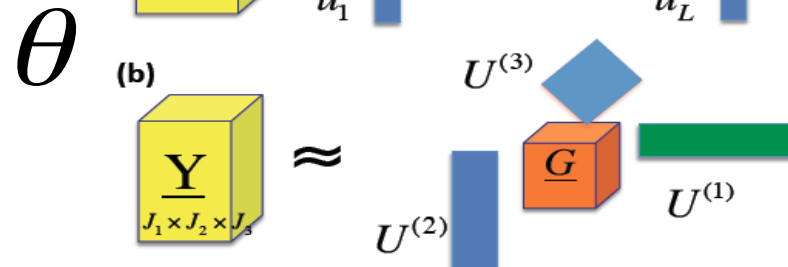


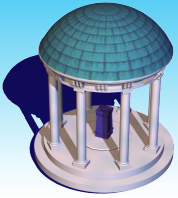
Zhou, Li, and Zhu (2013)
Li, Zhou, and Li (2013)

CP decomposition



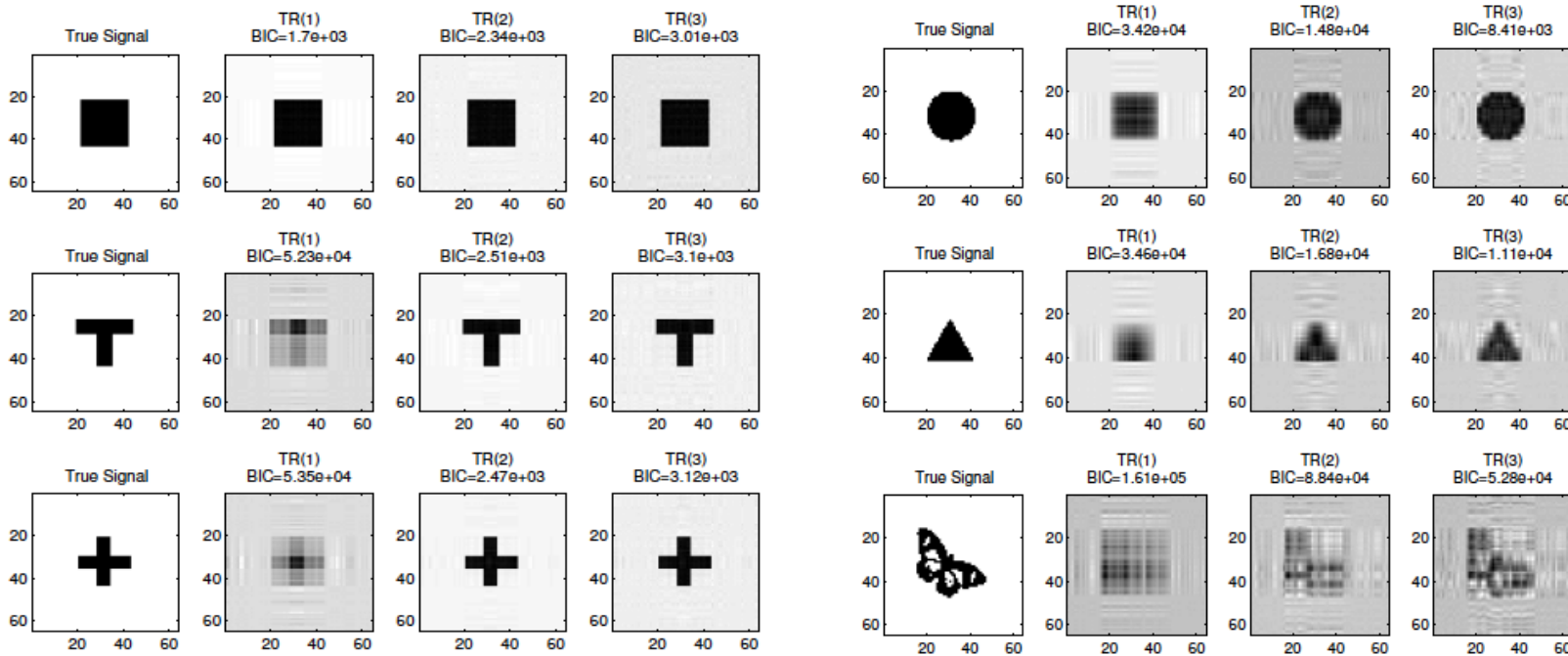
Tucker decomposition





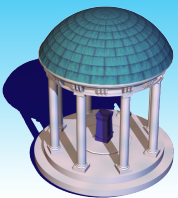
Scalar-on-Image Models

Simulations



Key Conditions:

- Tensor Approximation B
- Restricted space property for X and B



Scalar-on-Image Models

ADHD 200

Attention Deficit and Hyperactivity Disorder (ADHD) data
(http://fcon_1000.projects.nitrc.org/indi/adhd200/)

- ▶ 776 subjects: 491 normal controls and 285 combined ADHD subjects
- ▶ 442 males (average age: 11.98, sd: 3.14 years) and 287 females (average: 11.86, sd: 3.49)
- ▶ T1-weighted images were acquired and preprocessed by standard steps
- ▶ Segmentation: grey matter (GM), white matter (WM), ventricle (VN), and cerebrospinal fluid (CSF)

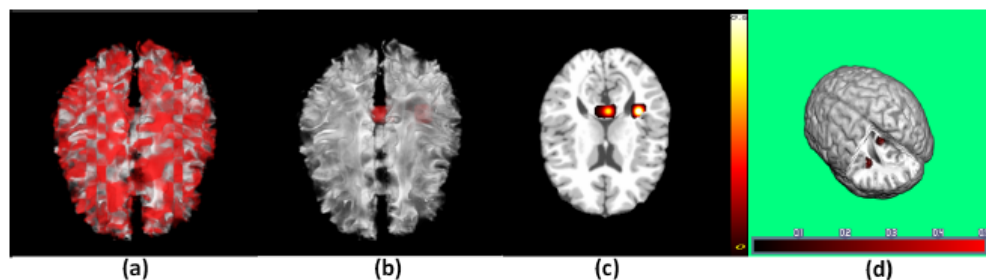
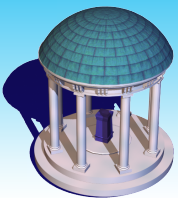


Figure: Panel (a) is the unpenalized estimate overlaid on a randomly selected subject; (b) is the regularized estimate; (c) is a selected slice of the regularized estimate overlaid on the template; and (d) is a 3D rendering of the regularized estimate.

- ▶ Two regions of interest: **left temporal lobe white matter** and **the splenium in the corpus callosum**



Scalar-on-Image Models

Strategy 2: Functional Approach

$$y_i = \theta_0 + \int_D \theta(d) X_i(d) m(d) + \varepsilon_i$$

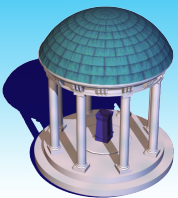


$$\theta(d) = \sum_{k=1}^{\infty} \theta_k \psi_k(d)$$

$$y_i = \theta_0 + \sum_{k=1}^{\infty} \theta_k \int_D \psi_k(d) X_i(d) m(d) + \varepsilon_i$$

Basis Methods: fixed and data-driven basis functions

$$K_{\theta} = \left\{ \theta(d) = \sum_{k=1}^{\infty} \theta_k \psi_k(d) : (\theta_1, \dots) \in \ell^2 \right\} \longleftrightarrow C(d, d') = \text{Cov}(X(d), X(d')) = \sum_{k=1}^{\infty} \lambda_k \psi_k(d) \psi_k(d')$$

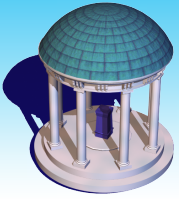


Key Conditions

Key Conditions: an **excellent** set of **basis functions**

- **Sparsity of** $\{\theta_k : k = 1, \dots\}$
- **Decay rate of spectral of** $C(d, d') = \text{Cov}(X(d), X(d'))$

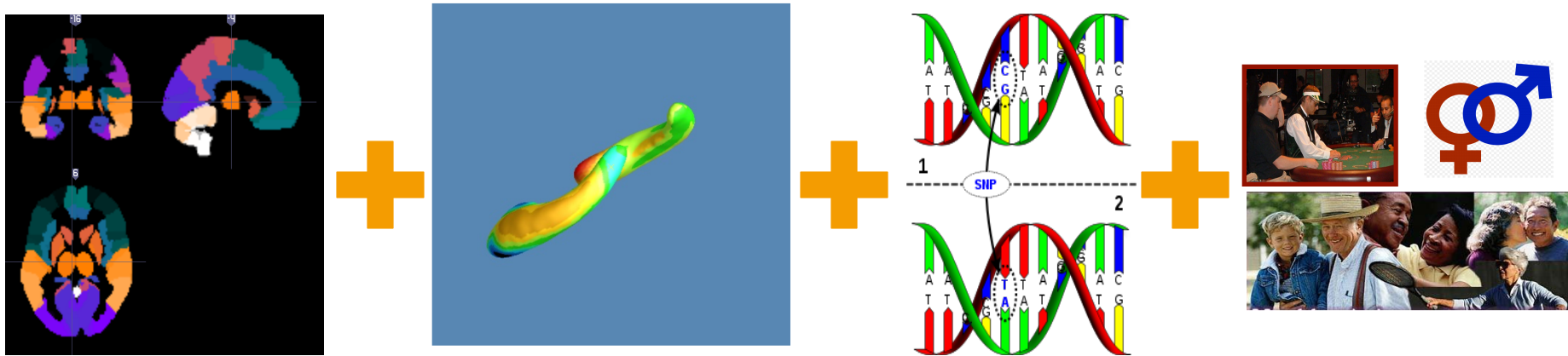
$$\theta(d) \approx \sum_{k=1}^K \theta_k \psi_k(d) \quad K \ll n$$



The ADNI data

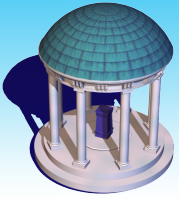
Mild Cognitive Impairment subjects

Interested in predicting the **timing of an MCI patient that converts to AD** by integrating the imaging data, the clinical variables, and genetic covariates.



Full Model: AUC=0.96

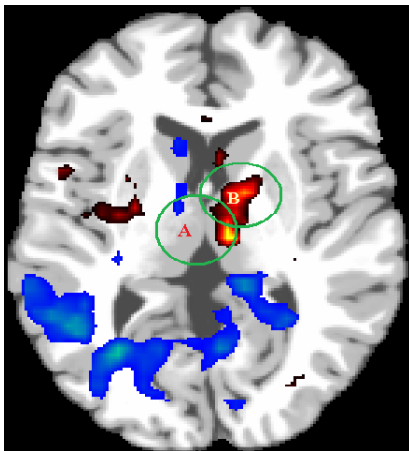
Partial Model: AUC=0.82



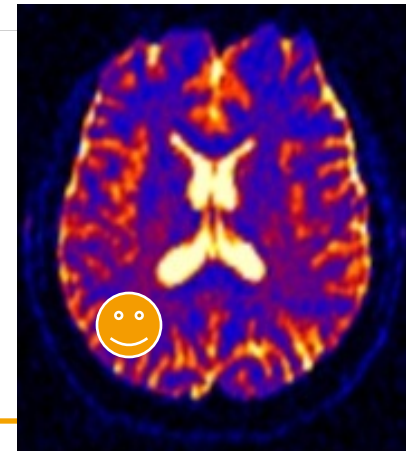
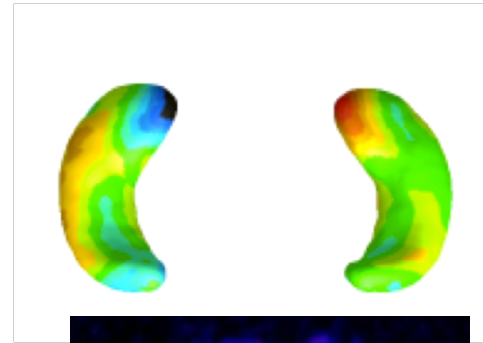
Limitations

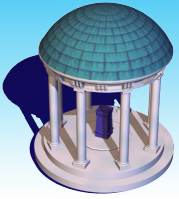
Is this **the right space** for statistical inference?

$$\{X_i(d) : d \in D\}$$



$$\left\{ \int_D \psi_k(d) X_i(d) m(d) : d \in D \right\}$$



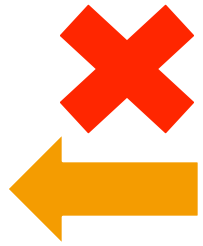


Rabbit and Wolf Story

$$\{y_i : i = 1, \dots, n\}$$

$$y_i = f_0(X_i) + \varepsilon_i$$

$$X_i = \{X_i(d) : d \in D\}$$



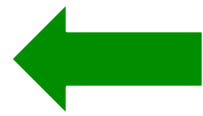
$$y_i = f(G_i) + \varepsilon_i$$

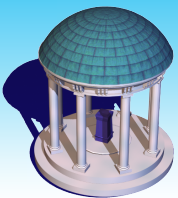


$$G_i = G\{\tilde{X}_i(d) : d \in D_0\}$$



$$\tilde{X}_i = \{\tilde{X}_i(d) : d \in D_0\}$$





Feature Space Determination

$$X_i = \{X_i(d) : d \in D\}$$



Splitting/Weighting methods

$$\tilde{X}_i = \{\tilde{X}_i(d) : d \in D_0\}$$



**Level sets
Factor Models**

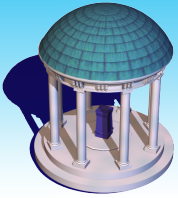
$$G_i = G\{\tilde{X}_i(d) : d \in D_0\}$$

Splitting

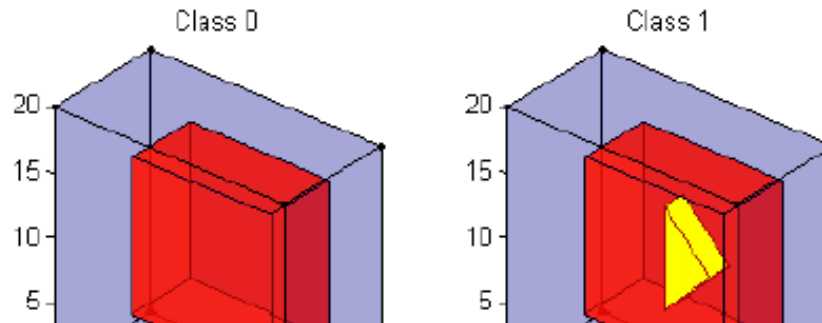
$$y_i = \theta_0 + \sum_k \int_{D_k} \theta(d) X_i(d) m(d) + \varepsilon_i$$

Weighting

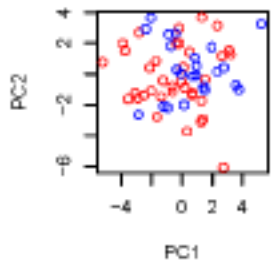
$$y_i = \theta_0 + \int_D \theta(d) w(d) X_i(d) m(d) + \varepsilon_i$$



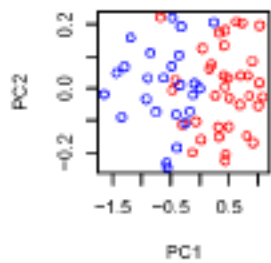
Spatially Weighted PCA



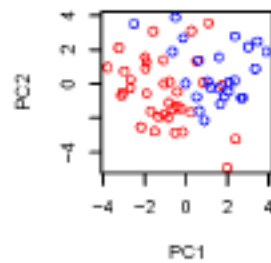
PCA : training



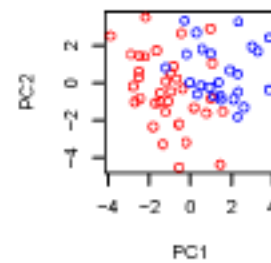
SPCA-50 : training



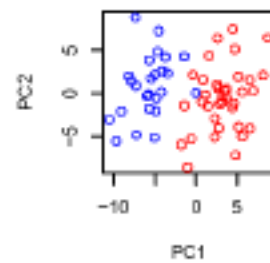
WPCA-1 : training



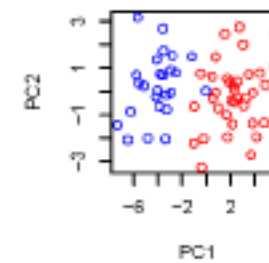
WPCA-2 : training



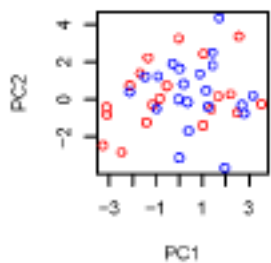
SWPCA : training



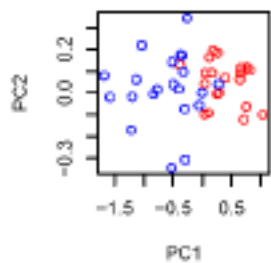
PSWPCA : training



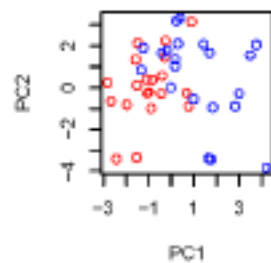
PCA : test



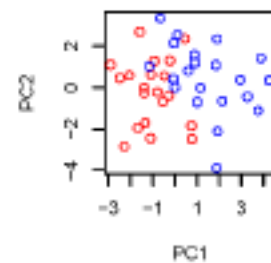
SPCA-50 : test



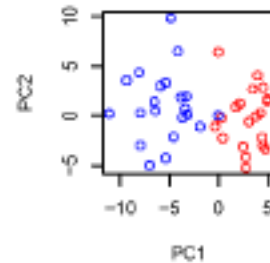
WPCA-1 : test



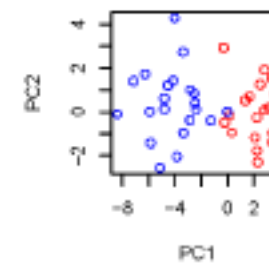
WPCA-2 : test

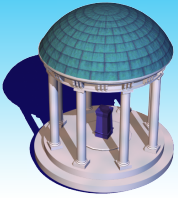


SWPCA : test



PSWPCA : test





Spatially Weighted PCA

Table 1: Average Misclassification Percentage for Simulation I

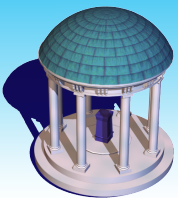
| | PCA | SPCA | | | | | WPCA-1 | WPCA-2 | SWPCA | PSWPCA |
|-------------|----------------|----------------|----------------|----------------|----------------|----------------|----------------|----------------|-----------------------|-----------------------|
| | ALL | 50 | 100 | 200 | 400 | 1000 | ALL | ALL | ALL | ALL |
| REG | .302 (.078) | .126 (.052) | .132 (.052) | .142 (.055) | .162 (.057) | .205 (.064) | .199 (.064) | .130 (.056) | .026 (.025) | .025 (.024) |
| k-NN | .338 (.071) | .135 (.049) | .141 (.049) | .152 (.050) | .182 (.053) | .225 (.071) | .186 (.055) | .156 (.059) | .030 (.029) | .027 (.025) |
| SVM | .327 (.078) | .140 (.054) | .147 (.055) | .159 (.055) | .183 (.059) | .226 (.072) | .215 (.067) | .152 (.055) | .033 (.029) | .028 (.026) |

Standard deviations are in parenthesis. For SPCA, the number of “top” selected voxels used in the algorithm are considered to be 50, 100, 200, 400, and 1000.

Table 2: Average Misclassification Percentage for Simulation I (Non-PCA Methods)

| SPLS-REG | SPLS-kNN | SPLS-SVM | SPLS | SDA |
|----------------|----------------|----------------|----------------|----------------|
| .130 (.052) | .139 (.056) | .156 (.066) | .128 (.050) | .120 (.050) |

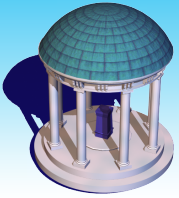
Standard deviations are in parenthesis.



Multiscale Factor Prediction Model

Hippocampal Surfaces Data Analysis

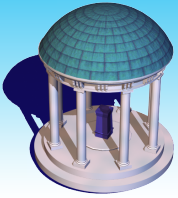
- Hippocampal surface data consist of the vector with the length 30,000 at the baseline for each subject.
- The first 15,000 parts of the vector were from the left location and the rest parts of it were from the right location.
- We use the diagnostic covariate (Alzheimer's disease VS Normal), gender and age as demographic information.
- We also use the APOE genotype variables since relevant studies have shown that the APOE4 genotype has significant effect on the subject.



Multiscale Factor Prediction Model

Hippocampal Surfaces Data Analysis

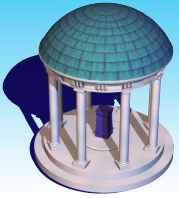
- Our goal is to predict the behavior score of the subject at the time when it is five year after the baseline.
- We had 406 individuals, 226 individuals for training and 180 individuals for test set, respectively.
- First, we estimated the number of the nonzero global coordinates as 500, 700 and 1000 cases where for each case, the half of each case was selected from the left and the rest was selected from the right.
- Next, we extracted the local information from the sequence of the correlation matrices.



Multiscale Factor Prediction Model

Table: Predictions for behavior score in hippocampal surfaces data.

| <i>ID</i> | Y_{true} | \hat{Y}_{1000} | \hat{Y}_{700} | \hat{Y}_{500} | <i>Age</i> | <i>Status</i> | <i>Gender</i> | <i>AP1</i> | <i>AP2</i> |
|-----------|------------|------------------|-----------------|-----------------|------------|---------------|---------------|------------|------------|
| 270 | 27.33 | 27.934 | 27.746 | 27.559 | 85.2 | 1 | 1 | 3 | 4 |
| 268 | 13.33 | 14.895 | 14.733 | 15.238 | 82.8 | 1 | 1 | 3 | 4 |
| 318 | 30.67 | 32.029 | 32.237 | 31.742 | 88.2 | 1 | 1 | 3 | 3 |
| 283 | 20 | 18.348 | 18.631 | 19.043 | 80.1 | 1 | 1 | 3 | 3 |
| 304 | 24 | 22.873 | 23.128 | 22.894 | 80.1 | 1 | 0 | 3 | 4 |
| 307 | 17.67 | 16.163 | 16.126 | 16.267 | 76.2 | 1 | 0 | 3 | 4 |
| 312 | 17.33 | 17.484 | 17.532 | 17.42 | 72.3 | 1 | 0 | 3 | 4 |
| 280 | 20.67 | 22.537 | 20.688 | 20.092 | 72 | 1 | 0 | 3 | 4 |
| 302 | 17.67 | 17.947 | 17.425 | 17.506 | 80.1 | 1 | 0 | 2 | 4 |
| 345 | 10.33 | 10.132 | 11.517 | 12.233 | 80.7 | 0 | 1 | 3 | 4 |
| 343 | 3.67 | 4.035 | 3.502 | 3.977 | 73.8 | 0 | 1 | 3 | 4 |
| 337 | 7.33 | 6.809 | 7.012 | 7.758 | 72.6 | 0 | 1 | 3 | 4 |
| 361 | 9.67 | 10.466 | 10.794 | 10.992 | 85.8 | 0 | 1 | 3 | 3 |
| 344 | 13 | 14.677 | 14.689 | 14.61 | 70.8 | 0 | 1 | 3 | 3 |
| 364 | 11 | 11.557 | 11.718 | 11.742 | 70.8 | 0 | 1 | 3 | 3 |
| 401 | 0.67 | 1.12 | 1.175 | 1.082 | 74.1 | 0 | 1 | 2 | 3 |
| 380 | 7 | 6.866 | 5.476 | 5.961 | 72.9 | 0 | 0 | 3 | 4 |
| 353 | 8.67 | 8.123 | 7.431 | 7 | 83.7 | 0 | 0 | 3 | 3 |

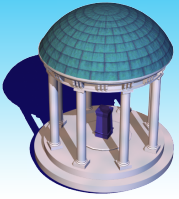


ASA: Statistics in Imaging Section

SAMSI

2013 Neuroimaging Data Analysis

2015-2016 Challenges in Computational Neuroscience



Acknowledgement

